Mathematical Modelling and Numerical Analysis Will be set by the publisher
Modélisation Mathématique et Analyse Numérique

ANALYSIS OF A MIMETIC FINITE DIFFERENCE APPROXIMATION OF FLOWS IN FRACTURED POROUS MEDIA

Luca Formaggia[1], Anna Scotti[2] and Federica Sottocasa[3]

Abstract. We consider the mixed formulation for Darcy's flow in fractured media. We give a well-posedness result that does not rely on the imposition of pressure in part of the boundary of the fracture network, thus including a fully immersed fracture network. We present and analyze a mimetic finite difference formulation for the problem, providing convergence results and numerical tests.

1991 Mathematics Subject Classification. 65N12, 65N99, 76S05.

September 12, 2018.

Introduction

It is well known that flow in porous media, in particular in the case of geophysical applications, is often characterized by very strong heterogeneities. In particular fractures, interfaces between different materials and faults have a major impact on the flow at all spatial scales. Indeed, due to the strong permeability contrasts, fractures and faults can act either as preferential paths for the flow, or as barriers forming pressure compartments.

In the past decades flow through fractured porous media has typically been simulated by means of dual porosity models [11]. However, this approach has some important limitations [33], in particular it is not adequate in the case of disconnected networks, or in the case of a small number of large fractures. For these reasons discrete fracture models, which represent fractures explicitly, are developing more and more.

Since fractures typically have a small aperture compared to their characteristic length, it is a common choice in the modelling of discrete fracture models to represent fractures as $d-1$-dimensional entities immersed in a d-dimensional domain, for instance, surfaces in three dimensional domains of lines in the two dimensional case. From the mathematical point of view a suitable geometrically reduced model should be then solved on such manifolds. Following the existing literature, we assume that fractures are filled by a porous medium with different porosity and permeability than the surrounding porous matrix, and that flow can be described by Darcy's law both in the bulk porous medium and in the fractures. However, we point out that if we consider fractures with porosity $\phi = 1$, but with small aperture, thanks to the parallel plates approximation [1] we obtain similar governing equations.

Keywords and phrases: Flow in porous media; Fracture networks; Mimetic finite difference

[1] MOX-Dip. di Matematica "F. Brioschi" Politecnico di Milano via Bonardi 9, 20133 Milano, Italy. luca.formaggia@polimi.it

[2] MOX-Dip. di Matematica "F. Brioschi" Politecnico di Milano via Bonardi 9, 20133 Milano, Italy. anna.scotti@polimi.it

[3] MOX-Dip. di Matematica "F. Brioschi" Politecnico di Milano via Bonardi 9, 20133 Milano, Italy. federica.sottocasa@mail.polimi.it

A reduced model for Darcy flow in fractures has been derived in [3] for the case of very permeable fractures, and later generalized to fractures with low permeability in [35]. More recently it has been extended to describe transport in fractured media [28], and two-phase flow, see [29,32].

Even if the use of a geometrically reduced model avoids the need for extremely refined or anisotropic grids inside the fractures, the construction of a computational grid for realistic cases is a challenging task (see, for instance, [24]): a fractured oil reservoir can be cut by several thousands of fractures, often intersecting or very close together. A computational grid conforming to the fractures can thus be characterized by very small elements and low quality, due to high aspect ratios and small angles. For most numerical methods the quality of the grid has an impact on the accuracy of the solution. For this reasons methods have been proposed to simplify fracture networks by means of local modifications of the fractures position and geometry, [34], since they are in any case affected by uncertainty, see [14]. Another possible strategy is to avoid geometric conformity, i.e. to allow fractures to cross the elements of a coarse and regular background grid. In this case, the presence of the interfaces can be accounted for by suitable enrichments of the finite element spaces, exploiting the eXtended Finite Element Method, see [31] [23]. We point out that some methods allow for partial nonconformity of the grids, i.e. for grids whose faces must be aligned with the fractures, while the nodes can be independent on the two sides: see for instance [16, 25].

The approach adopted in this work instead consists in adopting a numerical method that is robust even with highly distorted computational grids: the Mimetic Finite Difference (MDF) Method. This method, as well as the Virtual Element Method, which can be regarded as its evolution, is indeed known to preserve the quality of the solution for very general computational grids, with polygonal or polyhedral elements and high anisotropy. In recent years the use of MFD has grown considerably, thanks to their flexibility and ability to preserve important properties of the physical and mathematical model. MDF has been employed to simulate flow in networks of fractures, see [12, 13], and flows in fractured porous media [2, 10], with a primal and mixed formulation, respectively. It has been used also for quasilinear elliptic problems [9], as well as non-linear and control problems [5, 7, 8].

The present work can be considered in continuity with the strategy used in [10], but differs from the previous literature because a dual mixed formulation, discretized with the MFD method, is employed in the bulk medium as well as in the fractures. This requires a different splitting of the degrees of freedom for the fracture flux at the intersection, and the enforcement of suitable coupling conditions.

Even if the reduced model for fractures adopted in this work, originally presented in [3,35], has already been extensively used with different discretization techniques [6,17,23,25,29,30] some theoretical aspects are still not completely understood. In this work we aim at providing a proof of the well posedness of the Darcy's problem in dual mixed form in the presence of a fully immersed network of fracture, i.e. without requiring the imposition of pressure on part of the fracture network boundary. In this case the proof differs significantly from existing results, since the role of the coupling terms becomes fundamental. Indeed, the well posedness for the problem in mixed form has been established for the case of a single fracture crossing the domain in [35], assuming pressure is imposed on part of the fracture boundary, while the case of a fully immersed fracture is treated in [4], but using a primal formulation in the fracture. Finally, in [17] the authors analyze the case of a network, with a well-posedness result that extends to the case of fully immersed fractures, but using the primal formulation both in the bulk and in the network.

For the numerical discretization of the problem by means of mixed mimetic finite differences we will prove for the first time well-posedness and convergence for this class of problems. Moreover, as concerns the discrete problem, we will show how some hypothesis necessary for the well-posedness at continuous level can be relaxed at discrete level, and we will verify this result by means of numerical experiments.

The paper is organized as follows: in section 1 we present the governing equation for a single-phase flow in a fractured porous medium introducing some useful notation. In section 2 we introduce the weak formulation of the problem and prove its well-posedness. Section 3 is dedicated to the presentation of the numerical method and the proof of it stability and convergence. Some numerical experiments are shown in section 4, while section 5 is devoted to some concluding remarks.

1. The mathematical model

We describe the model we are considering for fluid flow in a fractured media.

1.1. The definition of the computational domain

We consider a bounded domain $\Omega \subset \mathbb{R}^d$, with $d = 2$ or 3, composed by a fractured porous medium. The set up of the mathematical model requires that Ω have a Lipschitz boundary, however we restrict the analysis to polytopal convex domains.

The fractures will be described as a collection of one co-dimensional planar manifolds, as shown in figure 1 for the two-dimensional case, following the model reduction strategy proposed in [3, 35].

With $\Gamma \in \mathbb{R}^{d-1}$ and $\Gamma \subset \Omega$ we denote a network formed by the union of N_Γ fractures γ_k, for $k = 1, \ldots, N_\Gamma$. Each γ_k is an open, bounded, planar $d-1$ dimensional manifold and we have

$$\Gamma = \bigcup_{k=1}^{N_\Gamma} \gamma_k.$$

Fractures can intersect only at their endpoints, i.e.

$$\forall\, j \neq k \quad \overline{\gamma}_k \cap \overline{\gamma}_j \,=\, \partial\gamma_k \cap \partial\gamma_j = i_{kj},$$

where i_{kj} is either the empty set (no intersections), or a point (in the 2D case) or a straight segment (in the 3D case). In particular, for the 3D setting we do not consider the case of fractures intersecting in a point.

We denote by $\mathcal{I}$ the set of all intersection points in the network, i.e. $\mathcal{I} = \cup i_{kj}$. To complete the definition of the network we follow the strategy proposed in [17]. We assume that, by suitably extending the fractures γ_k, we can partition Ω into a set of Lipschitz subdomains $\omega_\alpha \subset \Omega_\Gamma$, with $\alpha = 1, \ldots, N_\omega$ so that $\overline{\Omega} = \cup_1^{N_\omega} \overline{\omega}_\alpha$ and for each γ_k there are exactly two different values α_k^+ and α_k^- so that $\gamma_k \subset \partial\omega_{\alpha_k^+}$ and $\gamma_k \subset \partial\omega_{\alpha_k^-}$. This decomposition, shown in figure 2, allows us to identify the normal unitary vectors $\boldsymbol{n}_k^-$ and $\boldsymbol{n}_k^+$ to γ_k as those outwardly oriented with respect to $\omega_{\alpha_k^-}$ and $\omega_{\alpha_k^+}$, respectively. We define the (unique) normal to the fracture as $\boldsymbol{n}_k = \boldsymbol{n}_k^+ = -\boldsymbol{n}_k^-$, while $\boldsymbol{n}_\alpha$ will be used to indicate the outward normal to $\partial\omega_\alpha$. In the following $\boldsymbol{n}_\Gamma$ indicates the normal to Γ, i.e. $\boldsymbol{n}_\Gamma = \boldsymbol{n}_k$ on γ_k, for all k. Analogous definition for $\boldsymbol{n}_\Gamma^+$ and $\boldsymbol{n}_\Gamma^-$. Finally, for each ω_α we indicate with $\partial^\pm\omega_\alpha$ the portions of $\partial\omega_\alpha \cap \Gamma$ such that $\boldsymbol{n}_\alpha \cdot \boldsymbol{n}_\Gamma = \pm 1$, respectively. We set $\Omega_\Gamma = \Omega \setminus \overline{\Gamma}$ and we assume that its boundary can be partitioned into two measurable subsets $\partial\Omega^p$ and $\partial\Omega^u$, with $|\partial\Omega^p| > 0$.

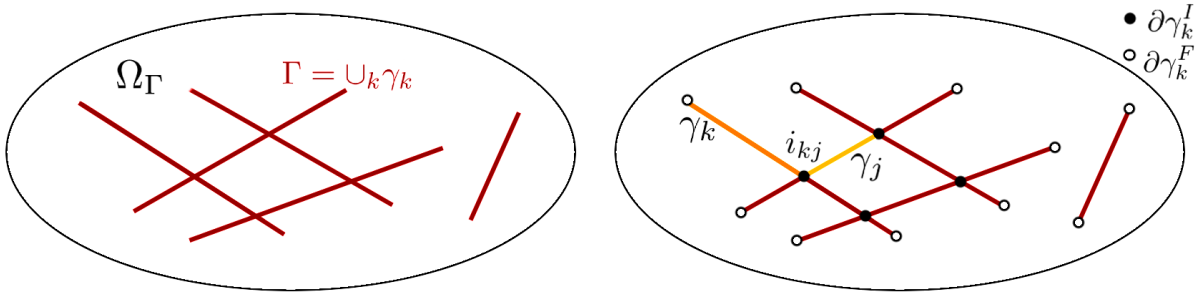

FIGURE 1. A two dimensional fracture network.

We can then subdivide the boundary of the fracture in different subsets (some of which may be empty). For each γ_k we divide its boundary in $\partial\gamma_k^p$ and $\partial\gamma_k^{\boldsymbol{u}}$ such that $\partial\gamma_k^p \cup \partial\gamma_k^u = \partial\gamma_k \cap \partial\Omega$. We then set $\partial\gamma_k^I = \partial\gamma_k \cap \mathcal{I}$ and $\partial\gamma_k^F = \partial\gamma_k \setminus \bigcup_{s=p,u,I} \partial\gamma_k^s$. For the 3D setting, one assumes that whenever $\partial\gamma_k^p$ or $\partial\gamma_k^u$ are not empty sets they have a strictly positive $d-2$ measure (in 2D they are just points).

For $s = p, u, F$ we define $I^s = \bigcup_{k=1}^{N_\Gamma} \partial\gamma_k^s$. Therefore, I^F contains the part of the boundary of Γ that is fully immersed in the domain Ω. If $I^p = I^u = \emptyset$ we have the case of a *fully immersed network*. Given an intersection point $i \in \mathcal{I}$ we denote with S_i the set of fractures γ_k that join in i.

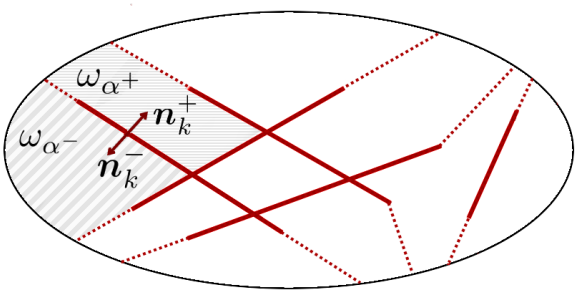

FIGURE 2. Decomposition of the domain.

In general, for given functions f_k defined on each γ_k we define $f = \prod_{k=1}^{N_\Gamma} \hat{f}_k$. We can now generalize the definition of average and jump of a function $f \in \Omega_\Gamma$ as

$$\{f\} = \frac{1}{2}(f^+ + f^-) \quad \text{and} \quad [\![f]\!] = f^+ - f^-,$$

where $f^\pm$ is the trace of f on $\Gamma^\pm = \bigcup_{k=1}^{N_\Gamma} \gamma_k^\pm$. With $\{f\}_k$ and $[\![f]\!]_k$ we denote the average and jump operators restricted to fracture γ_k.

Each γ_k is indeed an approximation of the actual fracture, which we assume can be described as

$$\tilde{\gamma}_k = \{\boldsymbol{y} \in \mathbb{R}^d : \boldsymbol{y} = \boldsymbol{x} + d\boldsymbol{n}_k,\, \boldsymbol{x} \in \gamma_k,\, d \in (-\frac{l_k(\boldsymbol{x})}{2}, \frac{l_k(\boldsymbol{x})}{2})\} \tag{1}$$

where l_k is the fracture aperture. We assume that l_k is a C^1 function and that there is a constant $l_* > 0$ such that $l_k > l_*$, for all k. We denote with $l_\Gamma = \prod_{k=1}^{N_\Gamma} l_k$ the aperture of the whole fracture network (note that it is in general discontinuous at the intersections). It is assumed that l_Γ be everywhere much smaller than the diameter of Ω, which justifies the use of a reduced $d-1$ dimensional model.

1.2. The model

We assume that the flow in the porous matrix and in the fractures be described by Darcy's law and by the mass conservation equation. We consider a single fluid with constant density and we neglect the effect of gravity. We employ the model that has been derived for a single fracture in [3,35], here extended to the case of a network.

We will indicate with $\boldsymbol{u}$ and p the Darcy macroscopic velocity and fluid pressure in the bulk domain Ω_Γ, while $\boldsymbol{K}$ is the permeability tensor in the bulk that, for the sake of simplicity, includes the dependence on the viscosity μ. The reduced problem for flow in the fracture has been obtained by integration of the governing equations across the fracture aperture, and by defining reduced variables for the flux $\hat{\boldsymbol{u}}$ and the average pressure $\hat{p}$ in each fracture. More precisely, if $\tilde{\boldsymbol{v}}_k : \gamma_k \to \mathbb{R}^d$ and $\tilde{p} : \gamma_k \to \mathbb{R}$ are the velocity and pressure in the actual fracture defined in (1), and $\boldsymbol{T}_k = \boldsymbol{I} - \boldsymbol{n}_k \otimes \boldsymbol{n}_k$ the projector on the tangent plane of fracture γ_k, where $\boldsymbol{I}$ here indicates the identity operator, we set

$$\hat{\boldsymbol{u}}_k = \int_{-\frac{l_k}{2}}^{\frac{l_k}{2}} \boldsymbol{T}_k \tilde{\boldsymbol{v}}_k, \quad \text{and} \quad \hat{p}_k = \frac{1}{l_k} \int_{-\frac{l_k}{2}}^{\frac{l_k}{2}} \tilde{p}_k,$$

and $\hat{\boldsymbol{u}} = \prod_{k=1}^{N_\Gamma} \hat{\boldsymbol{u}}_k$, while $\hat{p} = \prod_{k=1}^{N_\Gamma} p_k$.

We assume that the permeability (scaled by viscosity) in each fracture can be represented by a diagonal tensor in local (tangent and normal) coordinates. More precisely the permeability in the fractures can be uniquely decomposed as $\boldsymbol{K} = \hat{K}_n \boldsymbol{n}_\Gamma \otimes \boldsymbol{n}_\Gamma + \hat{\boldsymbol{K}}_\tau$, where on each γ_k $\hat{\boldsymbol{K}}_\tau$ is a tensor acting only on the planar manifold defined by γ_k, that is $\hat{\boldsymbol{K}}_\tau \boldsymbol{n}_\Gamma = \boldsymbol{0}$. Note that in the 2D setting $\hat{\boldsymbol{K}}_\tau = \hat{K}_\tau \boldsymbol{T}$, for a scalar function $\hat{K}_\tau$ defined on Γ, and $\boldsymbol{T} = \prod_{k=1}^{N_\Gamma} \boldsymbol{T}_k$.

We also define the following scaled quantities

$$\hat{\boldsymbol{K}} = l_\Gamma \hat{\boldsymbol{K}}_\tau \quad \text{and} \quad \eta = \frac{l_\Gamma}{\hat{K}_n}. \tag{2}$$

In fact, $\hat{\boldsymbol{K}}$ is an effective tangential permeability for the fracture, while η represents and effective conductivity. It is understood that when we write an operator on quantities defined on Γ we mean in fact the product of the corresponding operators on each γ_k. Additional assumptions on the parameters are reported in Section 2.2.

The complete coupled problem consists then of a Darcy problem in the bulk porous medium and a reduced Darcy problem in the fracture network,

$$\begin{cases} \operatorname{div} \boldsymbol{u} = f & \text{in } \Omega_\Gamma \\ \boldsymbol{K}^{-1}\boldsymbol{u} + \nabla p = 0 & \text{in } \Omega_\Gamma \\ p = g_p & \text{on } \partial\Omega^p \\ \boldsymbol{u}\cdot\boldsymbol{n} = g_u & \text{on } \partial\Omega^u \end{cases} \quad \text{and} \quad \begin{cases} \operatorname{div}_{\boldsymbol{\tau}} \hat{\boldsymbol{u}} = \hat{f} + [\![\boldsymbol{u}\cdot\boldsymbol{n}_\Gamma]\!] & \text{in } \Gamma \\ \hat{\boldsymbol{K}}^{-1}\hat{\boldsymbol{u}} + \nabla_{\boldsymbol{\tau}} \hat{p} = 0 & \text{in } \Gamma \\ \hat{\boldsymbol{u}}\cdot\boldsymbol{\tau} = \hat{g}_u & \text{on } I^u \\ \hat{\boldsymbol{u}}\cdot\boldsymbol{\tau} = 0 & \text{on } I^F \\ \hat{p} = \hat{g}_p & \text{on } I^p \end{cases} \tag{3}$$

complemented with the coupling conditions

$$\begin{cases} \eta\,\{\boldsymbol{u}\cdot\boldsymbol{n}_\Gamma\} = [\![p]\!] & \text{on } \Gamma \\ \eta\,\xi_0\,[\![\boldsymbol{u}\cdot\boldsymbol{n}_\Gamma]\!] = \{p\} - \hat{p} & \text{on } \Gamma \end{cases} \quad \text{and} \quad \begin{cases} \hat{p}_k = p_i & \text{in } i \quad \forall\, \gamma_k \in S_i, \quad \forall\, i \in \mathcal{I} \\ \sum\limits_{k:\,\gamma_k \in S_i} \hat{\boldsymbol{u}}_k|_i \cdot \boldsymbol{\tau}_k = 0 & \text{in } i \quad \forall\, i \in \mathcal{I} \end{cases} \tag{4}$$

where $\hat{p}_k$ e $\hat{\boldsymbol{u}}_k$ denote respectively pressure and flux in γ_k and p_i the pressure at the intersection point $i \in I$. While, $\boldsymbol{\tau}_k$ is the vector in the tangent plane of γ_k normal to $\partial\gamma_k$, and $\operatorname{div}_{\boldsymbol{\tau}}$ and $\nabla_{\boldsymbol{\tau}}$ indicate the tangent divergence and gradient operators, respectively.

Note that coupling conditions in (4) depend on a closure parameter ξ_0 that accounts for the assumption made on the pressure profile across the fracture aperture when deriving the reduced model. The assumption of a parabolic variation of fluxes (and thus cubic variation of pressure) across the fracture leads to the optimal value $\xi_0 = 1/12$. Its effect on the properties of the problem, and in particular its well posedness, will be discussed in the next section. Note that ξ_0 is related to the closure parameter ξ used in [35]: in particular, $\xi_0 = (2\xi - 1)/4$.

Remark 1.1. *We have imposed, on the immersed fracture tips, homogeneous conditions for the flux. This is quite standard in this type of problems. At the fracture intersection we have enforced pressure continuity and flux conservation: other possible, more general, conditions can be found in [26] or in [36]. Moreover, in the 3D setting, one may consider a more complex set of equations, accounting for flow along the intersection lines, as it has been proposed in [27] in the context of discrete fracture network simulations. A hierarchical approach that goes in that direction is also the one proposed in [16].*

2. Weak formulation and main analytic results

In this Section we will set up the weak formulation of the differential problem (3) with the coupling conditions (4). We will the analyze its well-posedness, focusing on the case where $I^p = \emptyset$, which encompasses the situation of a fully immersed network.

2.1. **Functional setting**

We will use standard notation for Lesbegue and Sobolev spaces. In particular for $p \in [1, \infty)$,

$$L^p(\Omega_\Gamma) = \{f : \Omega_\Gamma \to \mathbb{R} : \|f\|_{L^p(\Omega_\Gamma)} < \infty\},$$

with $\|f\|_{L^p(\Omega_\Gamma)} = \sqrt{\int_{\Omega_\Gamma} |f|^p d\Omega}$, while

$$L^\infty(\Omega_\Gamma) = \{f : \Omega_\Gamma \to \mathbb{R} : f \text{ measurable}, \|f\|_{L^\infty(\Omega_\Gamma)} < \infty\},$$

with $\|f\|_{L^\infty(\Omega_\Gamma)} = \text{supess}_{\boldsymbol{x}\in\Omega_\Gamma} |f(\boldsymbol{x})|$. We note that, being Γ a set of null d-measure, we can identify an element $L^p(\Omega_\Gamma)$ with an element of $L^p(\Omega)$, for any $p \in [1, \infty]$.

We indicate with $H^k(\Omega_\Gamma)$, for an integer $k > 0$, the space of functions whose restriction to any open and connected subset $\omega \subset \Omega_\Gamma$ is in $H^k(\omega)$. Indeed some configuration of the fracture network Γ can split Ω in disconnected parts. In this case $H^k(\Omega_\Gamma)$ is in fact a broken space. However, we can still formally write norms and inner products in the usual way. For instance, for any u and v in $H^1(\Omega_\Gamma)$

$$\|v\|_{H^1(\Omega_\Gamma)} = \left(\|v\|^2_{L^2(\Omega_\Gamma)} + \|\nabla v\|^2_{L^2(\Omega_\Gamma)}\right)^{1/2} \quad \text{and} \quad (u, v)_{H^1(\Omega_\Gamma)} = \int_{\Omega_\Gamma} (uv + \nabla u \cdot \nabla v)\, d\Omega.$$

We define

$$H_{\text{div}}(\Omega_\Gamma) = \{\boldsymbol{v} : \Omega_\Gamma \to \mathbb{R}^d : \|\boldsymbol{v}\|_{[L^2(\Omega_\Gamma)]^d} + \|\operatorname{div} \boldsymbol{v}\|_{L^2(\Omega_\Gamma)} < \infty\},$$

which is an Hilbert space equipped with the standard inner product

$$(\boldsymbol{u}, \boldsymbol{v})_{H_{\text{div}}(\Omega_\Gamma)} = \int_{\Omega_\Gamma} (\boldsymbol{u} \cdot \boldsymbol{v} + \operatorname{div}(\boldsymbol{u}) \operatorname{div}(\boldsymbol{v}))\, d\Omega.$$

For a full characterization of the spaces $H_{\text{div}}(\Omega_\Gamma)$ and $H^1(\Omega_\Gamma)$ the reader may refer, for instance, to [4].

For $p \in [1, \infty]$, we define, $L^p(\Gamma) = \prod_{k=1}^{N_\Gamma} L^p(\gamma_k)$, with standard norm for product spaces (and inner product in the case of L^2).

We now specify in more details the functional spaces we are adopting for our problem. For the velocity and pressure in the bulk we set the following spaces

$$\begin{aligned} &V^\Omega = \{\boldsymbol{v} \in H_{\text{div}}(\Omega_\Gamma) : \ [\![\boldsymbol{v} \cdot \boldsymbol{n}_\Gamma]\!] \in L^2(\Gamma), \{\boldsymbol{v} \cdot \boldsymbol{n}_\Gamma\} \in L^2(\Gamma), \boldsymbol{v} \cdot \boldsymbol{n}|_{\partial\Omega^u} = 0\}, \\ &M^\Omega = L^2(\Omega). \end{aligned} \tag{5}$$

Here we have used the short-hand notation $\boldsymbol{v} \cdot \boldsymbol{n}|_{\partial\Omega_{\boldsymbol{u}}}$ to indicate the trace on $\partial\Omega_{\boldsymbol{u}}$ of the normal component of the velocity. The space V^Ω is a Hilbert space when equipped with the norm

$$\|\boldsymbol{v}\|^2_{V^\Omega} = \|\boldsymbol{v}\|^2_{L^2(\Omega)} + \|\operatorname{div} \boldsymbol{v}\|^2_{L^2(\Omega)} + \|\{\boldsymbol{v} \cdot \boldsymbol{n}_\Gamma\}\|^2_{L^2(\Gamma)} + \|[\![\boldsymbol{v} \cdot \boldsymbol{n}_\Gamma]\!]\|^2_{L^2(\Gamma)}, \tag{6}$$

and the corresponding inner product

$$(\boldsymbol{v}, \boldsymbol{u})_{V^\Omega} = (\boldsymbol{v}, \boldsymbol{u})_{L^2(\Omega)} + (\operatorname{div} \boldsymbol{v}, \operatorname{div} \boldsymbol{u})_{L^2(\Omega)} + (\{\boldsymbol{v} \cdot \boldsymbol{n}_\Gamma\}, \{\boldsymbol{u} \cdot \boldsymbol{n}_\Gamma\})_{L^2(\Gamma)} + ([\![\boldsymbol{v} \cdot \boldsymbol{n}_\Gamma]\!], [\![\boldsymbol{u} \cdot \boldsymbol{n}_\Gamma]\!])_{L^2(\Gamma)}. \tag{7}$$

Remark 2.1. *Our definition of the space for the velocity in the bulk V^Ω differs from that used, for instance, in [35], were the authors introduced the norm*

$$|||\boldsymbol{v}|||^2_{V^\Omega} = \|\boldsymbol{v}\|^2_{L^2(\Omega)} + \|\operatorname{div} \boldsymbol{v}\|^2_{L^2(\Omega)} + \|\boldsymbol{v}^+ \cdot \boldsymbol{n}_\Gamma\|^2_{L^2(\Gamma)} + \|\boldsymbol{v}^- \cdot \boldsymbol{n}_\Gamma\|^2_{L^2(\Gamma)}.$$

However, it is immediate to verify that the two norms are equivalent. However, our definition turns out to be more convenient for the following derivations.

As for the fractures, we first define the spaces

$$H_{\rm div}(\gamma_k) = \{\hat{\boldsymbol{v}} \in L^2(\gamma_k) : {\rm div}_{\boldsymbol{\tau}}\, \hat{\boldsymbol{v}} \in L^2(\gamma_k)\},$$

with the corresponding canonical inner product and norm. Then,

$$\begin{array}{l} V^\Gamma = \{\hat{\boldsymbol{v}} \in \prod_{k=1}^{N_\Gamma} H_{\rm div}(\gamma_k) : \sum_{\gamma_k \in S_i} \hat{\boldsymbol{v}}_k \cdot \boldsymbol{\tau}_k|_i = 0,\ \forall i \in \mathcal{I},\ \hat{\boldsymbol{v}}_k \cdot \boldsymbol{\tau}_k|_{I^{\boldsymbol{u}}} = 0\} \\ M^\Gamma = L^2(\Gamma). \end{array} \tag{8}$$

We have adopted again the short hand notation of indicating with $\hat{\boldsymbol{v}}_k \cdot \boldsymbol{\tau}_k|_{I^{\boldsymbol{u}}}$ and $\hat{\boldsymbol{v}}_k \cdot \boldsymbol{\tau}_k|_i$ the trace of the normal components of the fracture velocity at the corresponding fracture boundary and intersection, respectively. More precisely condition $\sum_{\gamma_k \in S_i} \hat{\boldsymbol{v}}_k \cdot \boldsymbol{\tau}_k|_i = 0$ has to be interpreted as

$$\sum_{\gamma_k \in S_i} \int_{\gamma_k} q_k \big({\rm div}_{\boldsymbol{\tau}}\, \hat{\boldsymbol{v}}_k + \hat{\boldsymbol{v}}_k \cdot \nabla_{\boldsymbol{\tau}}\, q_k\big) = 0 \ \forall q_k \in H^1(\gamma_k) \text{ with } q_k = 0 \text{ on } \partial\gamma_k \cap \mathcal{I}.$$

The norm for V^Γ and M^Γ are given by

$$\|\hat{\boldsymbol{v}}\|^2_{V^\Gamma} = \sum_{k=1}^{N_\Gamma} \|\hat{\boldsymbol{v}}\|^2_{L^2(\gamma_k)} + \sum_{k=1}^{N_\Gamma} \|{\rm div}_{\boldsymbol{\tau}}\, \hat{\boldsymbol{v}}\|^2_{L^2(\gamma_k)}, \quad \|\hat{q}\|_{M^\Gamma} = \sum_{k=1}^{N_\Gamma} \|\hat{q}\|^2_{L^2(\gamma_k)}.$$

Finally we define the global spaces for velocity and pressure as follows,

$$\boldsymbol{W} = V^\Omega \times V^\Gamma, \quad \boldsymbol{M} = M^\Omega \times M^\Gamma, \tag{9}$$

and equip them with the canonical inner products and norms for product spaces. It is useful to introduce the affine spaces

$$V^\Omega_g = \boldsymbol{l}_g + V^\Omega, \quad V^\Gamma_g = \hat{\boldsymbol{l}}_g + V^\Gamma,$$

where $\boldsymbol{l}_g \in H_{\rm div}(\Omega_\Gamma)$ and $\hat{\boldsymbol{l}}_g \in H_{\rm div}(\Gamma)$ are suitable lifting of the velocity boundary data g_u and $\hat{g}_u$. We then set $\boldsymbol{W}_g = V^\Omega_g \times V^\Gamma_g$.

Remark 2.2. *For instance $\boldsymbol{l}_g$ may be set as the restriction on Ω_Γ of $\nabla\phi$ where ϕ satisfies $-\triangle\phi = 0$ in Ω, with $\frac{\partial\phi}{\partial n} = g_u$ on $\partial\Omega^u$ and $\phi = 0$ on $\partial\Omega^p$, while $\hat{\boldsymbol{l}}_g$ may be set as $\prod_{k=1}^{N_\Gamma} \nabla_\tau \psi_k$, where $-\nabla_\tau \psi_k = 0$ on γ_k, with $\frac{\partial \psi_k}{\partial \tau} = \hat{g}_u$ on $\partial\gamma_k^u$ and $\psi_k = 0$ on $\partial\gamma_k \setminus \partial\gamma_k^u$.*

Moreover, in the following it is understood that $H^k(\Gamma) = \prod_{k=1}^{N_\Gamma} H^k(\gamma_k)$, with standard inner product and norm for product spaces.

2.2. **Conditions on the data**

We make the following assumption on the data.

- $\boldsymbol{K}$ and $\hat{\boldsymbol{K}}$ are uniformly elliptic, i.e. there exists $0 < K_* \le K^*$ and $0 < \hat{K}_* \le \hat{K}^*$ so that, for all $\boldsymbol{t} \in \mathbb{R}^d$ and all $\hat{\boldsymbol{t}} \in \mathbb{R}^d$ with $\hat{\mathbf{t}} \cdot \boldsymbol{n}_\Gamma = 0$

$$K_*\|\boldsymbol{t}\|^2 \le \boldsymbol{t}^T \boldsymbol{K}(\boldsymbol{x})\boldsymbol{t} \le K^*\|\boldsymbol{t}\|^2 \text{ a.e. in } \Omega_\Gamma,\ \hat{K}_*\|\hat{\boldsymbol{t}}\|^2 \le \hat{\boldsymbol{t}}^T \hat{\boldsymbol{K}}(\boldsymbol{x})\hat{\boldsymbol{t}} \le \hat{K}^*\|\hat{\boldsymbol{t}}\|^2 \text{ a.e. in } \Gamma. \tag{10}$$

  Here $\|\cdot\|$ denotes the Euclidean norm.
- There exist $0 < \eta_* \le \eta^*$, such that

$$\eta_* \le \eta(\boldsymbol{x}) \le \eta^*, \quad \text{a.e. in } \Gamma. \tag{11}$$

- $f \in L^2(\Omega_\Gamma)$ and $\hat{f} \in L^2(\Gamma)$, while , $g_p \in H^{1/2}(\partial\Omega^p)$, $\hat{g}_p \in H^{1/2}(I^p)$, $g_u \in H^{-1/2}(\partial\Omega^u)$ and $\hat{g}_u \in H^{-1/2}(I^u)$.

We also set $\gamma_* = \min_k |\gamma_k|$ and $\gamma^* = \max_k |\gamma_k|$. Clearly, we assume that $\gamma_* > 0$ and this implies that the ratio $\frac{\max_k(|\gamma_k|)}{\min_k(|\gamma_k|)}$ is bounded from above.

In general, we will use a^* and a_* to indicate upper and lower bounds of variable a.

2.3. **Weak form**

We are now in the position of writing the weak form of Problem (3)-(4) and study its properties.
Find $(\boldsymbol{u}, \hat{\boldsymbol{u}}) \in \boldsymbol{W}_g$ *and* $(p, \hat{p}) \in \boldsymbol{M}$ *such that*

$$\begin{cases} A\big((\boldsymbol{u}, \hat{\boldsymbol{u}}), (\boldsymbol{v}, \hat{\boldsymbol{v}})\big) + B\big((\boldsymbol{v}, \hat{\boldsymbol{v}}), (p, \hat{p})\big) = F^u\big((\boldsymbol{v}, \hat{\boldsymbol{v}})\big), \\ B\big((\boldsymbol{u}, \hat{\boldsymbol{u}}), (q, \hat{q})\big) = F^p\big((q, \hat{q})\big), \end{cases} \tag{12}$$

for all $(\boldsymbol{v}, \hat{\boldsymbol{v}}) \in \boldsymbol{W}$ *and* $(q, \hat{q}) \in \boldsymbol{M}$. Here,

$$A\big((\boldsymbol{u}, \hat{\boldsymbol{u}}), (\boldsymbol{v}, \hat{\boldsymbol{v}})\big) = a(\boldsymbol{u}, \boldsymbol{v}) + \hat{a}(\hat{\boldsymbol{u}}, \hat{\boldsymbol{v}}), \tag{13}$$

where

$$a(\boldsymbol{u}, \boldsymbol{v}) = m(\boldsymbol{u}, \boldsymbol{v}) + c(\boldsymbol{u}, \boldsymbol{v}) = \int_{\Omega_\Gamma} (\boldsymbol{K}^{-1}\boldsymbol{u}) \cdot \boldsymbol{v}\, d\Omega + \int_\Gamma \eta\left(\{\boldsymbol{u} \cdot \boldsymbol{n}_\Gamma\}\{\boldsymbol{u} \cdot \boldsymbol{n}_\Gamma\} + \xi_0 [\![\boldsymbol{u} \cdot \boldsymbol{n}_\Gamma]\!][\![\boldsymbol{u} \cdot \boldsymbol{n}_\Gamma]\!]\right) d\gamma, \tag{14}$$

$$\hat{a}(\hat{\boldsymbol{u}}, \hat{\boldsymbol{v}}) = \int_\Gamma (\hat{\boldsymbol{K}}^{-1}\hat{\boldsymbol{u}}) \cdot \hat{\boldsymbol{v}}\, d\gamma, \tag{15}$$

and

$$B\big((\boldsymbol{v}, \hat{\boldsymbol{v}}), (q, \hat{q})\big) = b(\boldsymbol{v}, q) + \hat{b}(\hat{\boldsymbol{v}}, \hat{q}) + d(\boldsymbol{v}, \hat{q}), \tag{16}$$

where

$$b(\boldsymbol{v}, q) = -\int_\Omega \operatorname{div} \boldsymbol{v} q\, d\Omega, \quad \hat{b}(\hat{\boldsymbol{v}}, \hat{q}) = -\int_\Gamma \operatorname{div}_{\boldsymbol{\tau}} \hat{\boldsymbol{v}} \hat{q}\, d\gamma, \quad d(\boldsymbol{v}, \hat{q}) = \int_\Gamma [\![\boldsymbol{v} \cdot \boldsymbol{n}_\Gamma]\!] \hat{q}\, d\gamma. \tag{17}$$

The functionals at the right hand side collect the contributions of boundary and source terms, namely

$$F^u\big((\boldsymbol{v}, \hat{\boldsymbol{v}})\big) = -\int_{\partial\Omega_p} g_p \boldsymbol{v} \cdot \boldsymbol{n}\, d\gamma - \int_{I^p} \hat{g}_p \hat{\boldsymbol{v}} \cdot \boldsymbol{\tau}\, d\gamma, \quad F^p\big((q, \hat{q})\big) = -\int_\Omega f q\, d\Omega - \int_\Gamma \hat{f} \hat{q}\, d\gamma. \tag{18}$$

Here, $\boldsymbol{n}$ is the outward directed normal to Ω and $\boldsymbol{\tau}$ represents the outward normal to the network, i.e. on each γ_k, $\boldsymbol{\tau}$ is the unit vector normal to $\partial\gamma_k$ and laying on the plane defined by γ_k.

Remark 2.3. *For generality, we are writing our formulation referring to the 3D case. However, the previous expressions are valid also in the 2D setting provided some terms be interpreted correctly. For instance,* $\int_{I^p} \hat{g}_p \hat{\boldsymbol{v}} \cdot \boldsymbol{\tau}\, d\gamma$ *in the 2D setting has to be interpreted as* $\hat{g}_p(\boldsymbol{x})\hat{\boldsymbol{v}}(\boldsymbol{x}) \cdot \boldsymbol{\tau}(\boldsymbol{x})$ *for* $\boldsymbol{x} \in I^p$*, since in the 2D setting elements of* I^p *are points.*

2.4. **Well-posedness result**

We state now the main result of this Section.

Theorem 2.1. *Under the given assumptions on the data, problem* (12) *is well-posed if* Ω *is a convex polytope and under the condition* $\xi_0 > 0$.

In the proof we will consider only the case $I^p = \emptyset$, since it is the more complex to handle and with great interest for applications. The extension to the case where pressure is imposed on part of the fracture boundary is straightforward. This implies $F^u\big((\boldsymbol{v},\hat{\boldsymbol{v}})\big) = -\int_{\partial\Omega_p} g_p \boldsymbol{v}\cdot\boldsymbol{n}$, and $V_g^\Gamma = V^\Gamma$.

We also consider the case of homogeneous condition for the normal component of velocity in the bulk, i.e. $V_g^\Omega = V^\Omega$, since the more general case is recovered by standard lifting techniques as explained in 2.2. In this context the boundary data involves only g_P. We wish to note that in following we indicate with $a \lesssim b$ the existence of a positive constant C so that $a \leq Cb$. However, we will normally indicate explicitly constants that depend on the physical parameters of the problem.

The proof of Theorem 2.1 relies on a series of lemmas.

Lemma 2.1. *Forms A and B are bilinear and continuous on $\boldsymbol{W}\times\boldsymbol{W}$ and $\boldsymbol{W}\times\boldsymbol{M}$, respectively. F^u and F^p are linear and continuous functionals on $\boldsymbol{W}$ and $\boldsymbol{M}$, respectively.*

Proof. Linearity is an immediate consequence of the definition. Moreover, using Cauchy-Schwarz inequalities we can show that

$$\begin{aligned}|A\big((\boldsymbol{u},\hat{\boldsymbol{u}}),(\boldsymbol{v},\hat{\boldsymbol{v}})\big)| &\leq \max(K_*^{-1},\hat{K}_*^{-1},\eta^*,\xi_0\eta^*)\|(\boldsymbol{u},\hat{\boldsymbol{u}})\|_{\boldsymbol{W}}\|(\boldsymbol{v},\hat{\boldsymbol{v}})\|_{\boldsymbol{W}}\\ |B\big((\boldsymbol{v},\hat{\boldsymbol{v}}),(q,\hat{q})\big)| &\leq \|(\boldsymbol{v},\hat{\boldsymbol{v}})\|_{\boldsymbol{W}}\|(q,\hat{q})\|_{\boldsymbol{M}},\end{aligned}$$

while, by standard application of the Cauchy-Schwarz inequality,

$$|F^u\big((\boldsymbol{v},\hat{\boldsymbol{v}})\big)| \leq \|g_p\|_{L^2(\Omega)}\|(\boldsymbol{v},\hat{\boldsymbol{v}})\|_{\boldsymbol{W}},\quad |F^p\big((q,\hat{q})\big)| \lesssim (\|f\|_{L^2(\Omega)}+\|\hat{f}\|_{L^2(\Gamma)})\|(q,\hat{q})\|_{\boldsymbol{M}}.$$

□

Lemma 2.2. *If $\xi_0 > 0$ form A is coercive on the space $\boldsymbol{W}^0 = \{(\boldsymbol{v},\hat{\boldsymbol{v}})\in\boldsymbol{W}:\ B\big((\boldsymbol{v},\hat{\boldsymbol{v}}),(q,\hat{q})=0,\ \forall(q,\hat{q})\in\boldsymbol{M}\}$.*

Proof. The proof follows the technique illustrated in [35]. First of all we note that for elements of $\boldsymbol{W}^0$ we have $\operatorname{div}\boldsymbol{v}=0$ in $L^2(\Omega)$ and $\operatorname{div}_{\boldsymbol{\tau}}\hat{\boldsymbol{v}} = [\![\boldsymbol{v}\cdot\boldsymbol{n}_\Gamma]\!]$ in $L^2(\Gamma)$. Consequently, $\|(\boldsymbol{v},\hat{\boldsymbol{v}})\|_{\boldsymbol{W}}$ is equivalent to $\|\boldsymbol{v}\|_{L^2(\Omega)} + \|\hat{\boldsymbol{v}}\|_{L^2(\Gamma)} + \|\{\boldsymbol{v}\cdot\boldsymbol{n}_\Gamma\}\|_{L^2(\Gamma)} + \|[\![\boldsymbol{v}\cdot\boldsymbol{n}_\Gamma]\!]\|_{L^2(\Gamma)}$. Thus, by exploiting the properties of the problem parameters, we immediately have

$$A\big((\boldsymbol{v},\hat{\boldsymbol{v}}),(\boldsymbol{v},\hat{\boldsymbol{v}})\big) \gtrsim \min(\frac{1}{K^*},\frac{1}{\hat{K}^*},\eta_*,\xi_0\eta_*)\|(\boldsymbol{v},\hat{\boldsymbol{v}})\|^2_{\boldsymbol{W}},\ \forall(\boldsymbol{v},\hat{\boldsymbol{v}})\in\boldsymbol{W}^0 \tag{19}$$

□

Remark 2.4. *It may be proved that the condition $\xi_0 > 0$ is in fact also necessary for coercivity.*

Lemma 2.3. *Form B is inf-sup stable. In particular, there exist a constant $\beta > 0$ such that*

$$\inf_{(q,\hat{q})\in\boldsymbol{M}}\sup_{(\boldsymbol{v},\hat{\boldsymbol{v}})\in\boldsymbol{W}} B\big((\boldsymbol{v},\hat{\boldsymbol{v}}),(q,\hat{q})\big) \geq \beta\|(\boldsymbol{v},\hat{\boldsymbol{v}})\|_{\boldsymbol{W}}\|(q,\hat{q})\|_{\boldsymbol{M}}$$

It is here where the demonstration for the case of a fully immersed fracture (or in general $I^p=\emptyset$) differs substantially from that provided, for instance in [35] for a fracture with pressure imposed at the boundary. Indeed, here the role of the coupling term d is fundamental.

Proof. The inf-sup stability is equivalent to establish that there is a constant β so that, for any $(q,\hat{q})\in\boldsymbol{M}$ it is possible to find $(\boldsymbol{v},\hat{\boldsymbol{v}})\in\boldsymbol{W}$ so that

$$\begin{aligned}B\big((\boldsymbol{v},\hat{\boldsymbol{v}}),(q,\hat{q})\big) &= \|(q,\hat{q})\|^2_{\boldsymbol{M}},\\ \|(\boldsymbol{v},\hat{\boldsymbol{v}})\|_{\boldsymbol{W}} &\leq \frac{1}{\beta}\|(q,\hat{q})\|_{\boldsymbol{M}},\end{aligned} \tag{20}$$

Given $(q,\hat{q}) \in \boldsymbol{M}$ the proof consists of three steps.

Step one. We look for $\psi \in H^2(\Omega)$ weak solution of

$$\begin{cases} -\triangle\psi & = q \text{ in } \Omega, \\ \psi & = 0 \text{ on } \partial\Omega^p, \\ \frac{\partial\psi}{\partial n} & = 0 \text{ on } \partial\Omega^u. \end{cases} \tag{21}$$

The existence of the solution is guaranteed by the assumption of regularity on the domain Ω.

We set $\boldsymbol{v}_1 = \nabla\psi$ and $\hat{\boldsymbol{v}} = 0$. Now, the restriction of $\boldsymbol{v}_1$ in Ω_Γ is clearly in V^Ω with $[\![\boldsymbol{v}_1 \cdot \boldsymbol{n}]\!] = 0$ on Γ and we have

$$B\big((\boldsymbol{v}_1,\boldsymbol{0}),(q,\hat{q})\big) = \|q\|^2_{L^2(\Omega)}, \tag{22}$$

while

$$\|(\boldsymbol{v}_1,\boldsymbol{0})\|^2_{\boldsymbol{W}} = \|\nabla\psi\|^2_{L^2(\Omega)} + \|\triangle\psi\|^2_{L^2(\Omega)} + \|\{\boldsymbol{v}_1\cdot\boldsymbol{n}_\Gamma\}\|^2_{L^2(\Gamma)}.$$

Now, $\|\nabla\psi\|^2_{L^2(\Omega)} \lesssim \|q\|_{L^2(\Omega)}$ because of standard regularity result, $\|\triangle\psi\|^2_{L^2(\Omega)} = \|q\|_{L^2(\Omega)}$ by construction, while elliptic regularity and trace inequality for functions in $H^2(\Omega)$ allow us to state that $\|\{\boldsymbol{v}_1\cdot\boldsymbol{n}_\Gamma\}\|_{L^2(\Gamma)} \lesssim \|q\|_{L^2(\Omega)}$.

In conclusion,

$$\|(\boldsymbol{v}_1,\boldsymbol{0})\|_{\boldsymbol{W}} \lesssim \|q\|_{L^2(\Omega_\Gamma)}. \tag{23}$$

Step 2. For each fracture in the network we look of the function $\hat{\phi}_k \in H^1(\gamma_k)\setminus\mathbb{R}$ that solves

$$\begin{cases} -\triangle_\tau\hat{\phi}_k & = \hat{q}_k - \overline{q}_k \quad \text{in } \gamma_k, \\ \dfrac{\partial\hat{\phi}_k}{\partial\tau_{\gamma_k}} & = 0 \quad \text{on } \partial\gamma_k, \end{cases} \tag{24}$$

where $\overline{q}_k = |\gamma_k|^{-1}\int_{\gamma_k}\hat{q}_k$ and $\dfrac{\partial\hat{\phi}_k}{\partial\tau_{\gamma_k}} = \nabla_{\boldsymbol{\tau}}\,\hat{\phi}_k\cdot\boldsymbol{\tau}_k$, where we recall that $\boldsymbol{\tau}_k$ is the vector in the tangent plane of γ_k normal to $\partial\gamma_k$. We take $\hat{\boldsymbol{v}}_k = \nabla_{\boldsymbol{\tau}}\,\phi_k$. We note that, thanks to standard regularity results,

$$\|\hat{\boldsymbol{v}}_k\|^2_{H_{\mathrm{div}}(\gamma_k)} = \|\nabla_\tau\phi_k\|^2_{L^2(\gamma_k} + \|\triangle_\tau\phi_k\|^2_{L^2(\gamma_k)} \lesssim \|\hat{q}_k - \overline{q}_k\|^2_{L^2(\gamma_k)} \le \|\hat{q}_k\|^2_{L^2(\gamma_k)} + |\gamma_k|\overline{q}_k^2.$$

Since $|\gamma_k|\overline{q}_k^2 = |\gamma_k|^{-1}(\int_{\gamma_k}\hat{q}_k)^2 \le \|\hat{q}_k\|^2_{L^2(\gamma_k)}$, we conclude that

$$\|\hat{\boldsymbol{v}}_k\|_{H_{\mathrm{div}}(\gamma_k)} \lesssim \|\hat{q}_k\|_{L^2(\gamma_k)} \tag{25}$$

We now set $\hat{\boldsymbol{v}} = \prod_{k=1}^{N_\Gamma}\hat{\boldsymbol{v}}_k$, it is immediate to verify that it belongs to V^Γ and that $\|\hat{\boldsymbol{v}}\|_{V^\Gamma} \lesssim \|\hat{q}\|_{M^\Gamma}$, and thus

$$\|(\boldsymbol{0},\hat{\boldsymbol{v}})\|_{\boldsymbol{W}} \lesssim \|(q,\hat{q})\|_{\boldsymbol{M}}. \tag{26}$$

Furthermore, we have

$$B\big((\boldsymbol{0},\hat{\boldsymbol{v}}),(q,\hat{q})\big) = \|\hat{q}\|^2_{L^2(\Gamma)} - \sum_{k=1}^{N_\Gamma}|\gamma_k|\overline{q}_k^2. \tag{27}$$

Step 3. We define on each fracture γ_k two "flux carriers" z_k^+ and z_k^- (see figure 3) so that

$$[\![z_k]\!]_k = z_k^+ - z_k^- = \overline{q}_k, \tag{28}$$

while the averages $\{z_k\} = \frac{z_k^+ + z_k^-}{2}$ minimize

$$J = \sum_{k=1}^{N_\Gamma}|\gamma_k|^2\{z_k\}^2$$

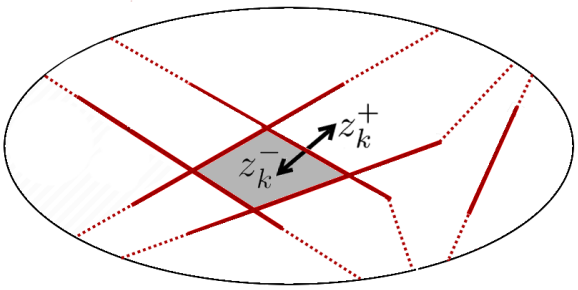

FIGURE 3. Definition of the flux carriers.

under the condition that for all ω_α such that $\partial\omega_\alpha \cap \partial\Omega^p = \emptyset$ we have

$$\sum_{\gamma_k \subset \partial^+\omega_\alpha} |\gamma_k| z_k^+ - \sum_{\gamma_k \subset \partial^-\omega_\alpha} |\gamma_k| z_k^- = 0. \tag{29}$$

We note that the problem admits a solution, because of the Euler formula connecting the number of faces in a polyhedral mesh, and the fact that there is at least a ω_α such that $\partial\omega_\alpha \cap \partial\Omega^p \neq \emptyset$. Furthermore, since

$$z_k^+ = \{z_k\}_k + \frac{1}{2}[\![z_k]\!]_k, \text{ and } z_k^- = \{z_k\}_k - \frac{1}{2}[\![z_k]\!]_k, \tag{30}$$

equation (29) may be rewritten as

$$\sum_{\gamma_k \subset \partial^+\omega_\alpha} |\gamma_k| \{z_k\}_k - \sum_{\gamma_k \subset \partial^-\omega_\alpha} |\gamma_k| \{z_k\}_k = -\frac{1}{2} \sum_{\gamma_k \subset \partial\omega_\alpha} |\gamma_k| [\![z_k]\!]_k,$$

and, as we are looking for the minimum of J, the solution satisfies

$$\sum_{k=1}^{N_\Gamma} |\gamma_k|^2 \{z_k\}_k^2 \lesssim \sum_{k=1}^{N_\Gamma} |\gamma_k|^2 [\![z_k]\!]_k^2 = \sum_{k=1}^{N_\Gamma} |\gamma_k|^2 \overline{q}^2 \leq \sum_{k=1}^{N_\Gamma} |\gamma_k| \|\hat{q}_k\|^2_{L^2(\gamma_k)} \leq \max_k(|\gamma_k|) \|\hat{q}\|^2_{L^2(\Gamma)},$$

and, consequently,

$$\sum_{k=1}^{N_\Gamma} |\gamma_k| \{z_k\}^2 \lesssim \frac{\max_k(|\gamma_k|)}{\min_k(|\gamma_k|)} \|\hat{q}\|^2_{L^2(\Gamma)}. \tag{31}$$

Condition (29) is necessary to equilibrate the fluxes in the ω_α that do not have part pressure is imposed on the part of the boundary. Indeed, we now define the spaces

$$V_\alpha = \begin{cases} H^1(\omega_\alpha) & \text{if } \partial\omega_\alpha \cap \partial\Omega^p \neq \emptyset, \\ H^1(\omega_\alpha) \setminus \mathbb{R} & \text{if } \partial\omega_\alpha \cap \partial\Omega^p = \emptyset, \end{cases}$$

and consider the following problems:
For each ω_α find $\psi_\alpha \in V_\alpha$ solution of

$$\begin{cases} -\triangle\psi_\alpha &= 0 & \text{in } \omega_\alpha \\ \dfrac{\partial\psi_\alpha}{\partial n} &= z_k^+ & \text{on } \partial^+\omega_\alpha \cap \gamma_k, \\ \dfrac{\partial\psi_\alpha}{\partial n} &= -z_k^- & \text{on } \partial^-\omega_\alpha \cap \gamma_k, \\ \dfrac{\partial\psi_\alpha}{\partial n} &= 0 & \text{on } \partial\omega_\alpha \setminus \partial\Omega^p, \\ \psi_\alpha &= 0 & \text{on } \partial\omega_\alpha \cap \partial\Omega^p. \end{cases} \tag{32}$$

Note that some of the boundary sets may be empty. We then set $\mathbf{v}_\alpha = \nabla\psi_\alpha$ and $\mathbf{v}_2 = \prod_{\alpha=1}^{N_\omega} \mathbf{v}_\alpha$. We have that on each γ_k

$$[\![\mathbf{v}_2 \cdot \boldsymbol{n}_\Gamma]\!]_k = \nabla\psi_{\alpha_k^+}|_{\gamma_k} \cdot \boldsymbol{n}_\Gamma - \nabla\psi_{\alpha_k^+}|_{\gamma_k} \cdot \boldsymbol{n}_\Gamma = \nabla\psi_{\alpha_k^+}|_{\gamma_k} \cdot \boldsymbol{n}_{\alpha_k^+} + \nabla\psi_{\alpha_k^+}|_{\gamma_k} \cdot \boldsymbol{n}_{\alpha_k^-} = [\![z_k]\!] = \overline{q}_k,$$

because of the definition of $\omega_{\alpha_k}^\pm$ and of $z_k^\pm$. While, $\{\mathbf{v}_2 \cdot \boldsymbol{n}_\Gamma\}_k = \{z_k\}_k$. Thus,

$$\|[\![\boldsymbol{v}_2 \cdot \boldsymbol{n}_\Gamma]\!]\|^2_{L^2(\Gamma)} = \sum_{k=1}^{N_\Gamma} |\gamma_k| [\![\mathbf{v}_2 \cdot \boldsymbol{n}_\Gamma]\!]_k^2 = \sum_{k=1}^{N_\Gamma} |\gamma_k| \overline{q}_k^2 \leq \|\hat{q}\|^2_{L^2(\Gamma)} \tag{33}$$

while, by exploiting (31), we have

$$\|\{\boldsymbol{v}_2 \cdot \boldsymbol{n}_\Gamma\}\|^2_{L^2(\Gamma)} = \sum_{k=1}^{N_\Gamma} |\gamma_k| \{\boldsymbol{v}_2 \cdot \boldsymbol{n}_\Gamma\}_k^2 = \sum_{k=1}^{N_\Gamma} |\gamma_k| \{z_k\}_k^2 =\lesssim \frac{\max_k(|\gamma_k|)}{\min_k(|\gamma_k|)} \|\hat{q}\|^2_{L^2(\Gamma)}. \tag{34}$$

A standard regularity result for problems (32) allows us to write

$$\|\nabla\psi_\alpha\|^2_{L^2(\omega_\alpha)} \lesssim \sum_{\gamma_k \subset \partial^+\omega_\alpha} |\gamma_k| (z_k^+)^2 + \sum_{\gamma_k \subset \partial^-\omega_\alpha} |\gamma_k| (z_k^-)^2,$$

and by summing over all α, using (30) and (31) as well the results implied in (33) and (34) we obtain

$$\sum_{\alpha=1}^{N_\omega} \|\nabla\psi_\alpha\|^2_{L^2(\omega_\alpha)} \lesssim \frac{\max_k(|\gamma_k|)}{\min_k(|\gamma_k|)} \|\hat{q}\|^2_{L^2(\Gamma)}.$$

and therefore we can conclude that

$$\begin{aligned} &B\big((\boldsymbol{v}_2, \mathbf{0}), (q, \hat{q})\big) = \sum_{k=1}^{N_\Gamma} |\gamma_k| \overline{q}_k^2, \\ &\|(\boldsymbol{v}_2, \mathbf{0})\|^2_{\boldsymbol{W}} = \|\boldsymbol{v}_2\|^2_{V^\Omega} = \sum_{\alpha=1}^{N_\omega} \|\nabla\psi_\alpha\|^2_{L^2(\omega_\alpha)} + \sum_{\alpha=1}^{N_\omega} \|\triangle\psi_\alpha\|^2_{L^2(\omega_\alpha)} + \sum_{k=1}^{N_\Gamma} |\gamma_k| \{z_k\}_k^2 + \sum_{k=1}^{N_\Gamma} |\gamma_k| [\![z_k]\!]_k^2 \lesssim \|\hat{q}\|^2_{L^2(\Gamma)}, \end{aligned} \tag{35}$$

where the hidden constant in the inequality depends also on the ratio of the maximum and minimum fracture measure.

The proof is concluded by taking $(\boldsymbol{v}, \hat{\boldsymbol{v}}) = (\boldsymbol{v}_1 + \boldsymbol{v}_2, \hat{\boldsymbol{v}})$ and noting that by collecting (22),(23),(26),(27) and (35), using the bilinearity of B and the subadditive property of norms, we obtain (20), where the positive constant β depends on the ratio $\min_k(|\gamma_k|)/\max_k(|\gamma_k|)$. □

Proof of Theorem 2.1. Thanks to Lemmas 2.1, 2.2 and 2.3, the proof is a standard result of saddle point problems, see for instance [15]. □

Remark 2.5. *Note that the construction of the flux carriers is not necessary if pressure is imposed on part of the fracture boundary, since it is possible to construct a coercive Poisson problem in the fracture network where the right hand side consists only of $\hat{q}$, using the strategy illustrated, for instance, in [26]. Yet, the given proof can be readily extended also to cover this case.*

3. Mimetic discretization

We present the mimetic discretization of problem (12). As done in the continuous setting, for generality we present for the case of $\Omega \subset \mathbb{R}^d$, d being equal to 3 or 2, even if the numerical experiments in this work have been carried out only for the 2D case. The terminology is that of the three-dimensional setting both in the bulk and in the fracture. For instance, in 3D a face of the bulk mesh is a two dimensional planar surface, while a face in the mesh for the fracture network is a 1D segment. In the two dimensional setting, the term face indicates a particular line segment in the bulk mesh and a point in the fracture mesh. Some of the terms used in the following have to be "reinterpreted" in the 2D case, where the fracture network is in fact one-dimensional.

3.1. **Mesh entities**

We consider a partition of Ω_Γ into a grid of d-dimensional polytopal cells $\mathcal{C}^\Omega = \{c_1, \ldots, c_{N^\Omega}\}$ while Γ is partitioned into a mesh of $d-1$-dimensional polytopal cells, $\mathcal{C}^\Gamma = \{\hat{c}_1, \ldots, \hat{c}_{N^\Gamma}\}$. We assume that the two meshes are conforming. More precisely each fracture cell $\hat{c}$ if geometrically congruent with the face of two bulk cells in $\mathcal{C}^\Omega$, each at the two opposite side of the fracture. This requirement is not a major limitation thanks to the flexibility offered by polyhedral grids.

We assume that both meshes satisfy the requirements stated in [22], which we recall for completeness.

First of all we define $h_c = \operatorname{diam}(c)$ and $h = \max_{c\in\mathcal{C}^\Omega} h_c$, while, $h_{\hat{c}} = \operatorname{diam}(\hat{c})$. Since the fracture mesh conforms to that in the bulk, we have $h_c \leq h$ and $h_{\hat{c}} \leq h$, for all $c \in \mathcal{C}^\Omega$ and $\hat{c} \in \mathcal{C}^\Gamma$.

We assume that $\mathcal{C}^\Omega$ and $\mathcal{C}^\Gamma$ belong to a family of meshes $\mathcal{M}_h$ parametrized with h. Any couple of meshes $(\mathcal{C}^\Omega, \mathcal{C}^\Gamma) \in \mathcal{M}_h$ admits conforming sub-partitions T_h^Ω and T_h^Γ composed by d-dimensional and $d-1$ dimensional simplexes, respectively, and their cells $c \in \mathcal{C}^\Omega$ and $\hat{c} \in \mathcal{C}^\Gamma$ have the following properties:

- A1 they may be decomposed into regular meshes T_c^Ω and $T_{\hat{c}}^\Gamma$ made of at most N_s simplexes that contain all vertices of the respective cells, where N_s is independent of h. We also assume that all elements of those sub-meshes are uniformly shape regular, i.e. the ratio of their diameter and the the ration of the maximal inscribed ball is bounded from above by a positive constant independent of h;
- A2 they are star shaped with respect to a point in their interior and each face at their boundary is also star shaped with respect to a point in its interior.

As a consequence of A1 we have that

$$h_c \max_{f\in\partial c} |f| \lesssim |c| \quad \text{and} \quad h_{\hat{c}} \max_{\hat{f}\in\partial \hat{c}} |\hat{f}| \lesssim |\hat{c}| \tag{36}$$

The set of faces at the boundary of cells in $\mathcal{C}^\Omega$ may be subdivided into the following subsets:

- The set of internal faces $\mathcal{F}_I^\Omega$, i.e. faces whose interior is contained in Ω_Γ. As customary, we assume that each $f \in \mathcal{F}_I^\Omega$ is shared by exactly two cells of $\mathcal{C}^\Omega$, indicated in the following by $c^+(f)$ and $c^-(f)$. Each face f has a unique orientation, defined by the unit normal vector $\boldsymbol{n}_f$. The outward normal of face f at the boundary of cell c is indicated by $\boldsymbol{n}_{c,f}$. We set $\alpha_{c,f} = \boldsymbol{n}_{c,f} \cdot \boldsymbol{n}_f$ and, by convention $\alpha_{c^\pm(f),f} = \pm 1$.
- The set of faces of cells in $\mathcal{C}^\Omega$ whose interior lay on Γ, here indicated by $\mathcal{F}_\Gamma^\Omega$. Since we are using a mesh conforming on Γ, the set $\mathcal{F}_\Gamma^\Omega$ is formed by pairs of faces f^+ and f^- geometrically identical but with opposite orientation. By convention, we assume that f^+ is oriented in accordance with the normal to the fracture $\boldsymbol{n}_\Gamma$.

- The set of faces at the boundary, subdivided into $\mathcal{F}^{\partial\Omega^u}$ and $\mathcal{F}^{\partial\Omega^p}$, such that $\cup_{f\in\mathcal{F}^{\partial\Omega^u}} f = \partial\Omega_u$ and $\cup_{f\in\mathcal{F}^{\partial\Omega^p}} f = \partial\Omega_p$. By convention, those faces are oriented conforming to the orientation of $\partial\Omega$, i.e. for those faces $\boldsymbol{n}_f$ is directed outwards w.r.t Ω.

As for the fracture network Γ we have adopted a discretization conforming to that of the bulk, thus for each $\hat{c} \in \mathcal{C}^\Gamma$ there are exactly two faces, $f^+(\hat{c})$ and $f^-(\hat{c})$, of $\mathcal{F}^\Omega_\Gamma$ geometrically identical to $\hat{c}$, but with opposite orientation. These faces are at the boundary of two cells of the bulk mesh, which we indicate with $c^+(\hat{c})$ and $c^-(\hat{c})$, respectively. Furthermore, for each $f \in \mathcal{F}^\Omega_\Gamma$ there is one and only one corresponding $\hat{c} = \hat{c}(f) \in \mathcal{C}^\Gamma$.

The set $\mathcal{F}^\Gamma$ is built as the union of the faces at the boundary of the cells in $\mathcal{C}^\Gamma$. The faces on the fracture intersection are repeated, one for each fracture γ_k meeting at the intersection. We can then subdivide $\mathcal{F}^\Gamma$ into

- internal faces $\mathcal{F}^\Gamma_I$, shared exactly by two cells, which are indicated by $\hat{c}^+(\hat{f})$ and $\hat{c}^-(\hat{f})$;
- intersection faces, i.e. those laying at the intersection among fractures, which, to implement the interface condition correctly, are grouped as follows. We define the set $\mathcal{F}^\#_\Gamma = \{F_1, F_2, \ldots\}$ whose generic element F_i represents the set of faces of $\mathcal{F}^\Gamma$ that are geometrically identical and belong to the boundary of different fracture cells of the network meeting at an intersection. For any $F \in \mathcal{F}^\#_\Gamma$ and for each $\hat{f} \in F$ we indicate with $\hat{c}(\hat{f})$ the cell such that $\hat{f} \in \partial\hat{c}$.
- boundary faces, further subdivided into $\mathcal{F}^{I^u} = \{\hat{f} \in \mathcal{F}^\Gamma : \hat{f} \in I^u\}$, $\mathcal{F}^{I^p} = \{\hat{f} \in \mathcal{F}^\Gamma : \hat{f} \in I^p\}$ and $\mathcal{F}^{I^F} = \{\hat{f} \in \mathcal{F}^\Gamma : \hat{f} \in I^F\}$. It is understood that some of these sets may be empty, and that $\cup_{\hat{f}\in\mathcal{F}^{I^u}} \hat{f} = I^u$, while $\cup_{\hat{f}\in\mathcal{F}^{I^p}} \hat{f} = I^p$.

In the case of immersed fractures, $\mathcal{F}^{I^u} = \mathcal{F}^{I^p} = \emptyset$ and $\cup\mathcal{F}^{I^F} = \partial\Gamma$.

In the following we use the pedix c, or $\hat{c}$ to indicate cell values, and f, or $\hat{f}$ for face values. We also make the following simplifying assumption on the data and on the mesh. We assume that $\boldsymbol{K}_c$ $\hat{\boldsymbol{K}}_{\hat{c}}$ and $\eta_{\hat{c}}$ are piecewise constant on a partition of the relative domain of definition, and that $\mathcal{C}^\Omega$ and $\mathcal{C}^\Gamma$ are conformal with the partition. This means that $\boldsymbol{K}$ $\hat{\boldsymbol{K}}$ and η are constant on each c (or $\hat{c}$). This assumption is made to simplify the exposition and the analysis, in a more general setting one may approximate those parameters with cell-wise constant functions $\boldsymbol{K}_c$ $\hat{\boldsymbol{K}}_{\hat{c}}$ and $\eta_{\hat{c}}$ by taking, for instance, the average value.

Finally, for the sake of notation, we will omit to indicate the Lesbegue measure in the integrals, e.g. $\int_{\Omega_\Gamma} f d\Omega$ will be simply written $\int_{\Omega_\Gamma} f$, unless ambiguity may arise.

3.2. **Mimetic degrees of freedom and projection operators**

As usual in mimetic formulation of differential problems, we need to locate the degrees of freedom for velocity and pressure in an appropriate way. Since we are planning to adopt a low order discretization method we will consider for the pressure in the bulk and in the fractures one degree of freedom for each element in $\mathcal{C}^\Omega$ and $\mathcal{C}^\Gamma$, respectively, While, one degree of freedom is associated to each element of $\mathcal{F}^\Omega$ and $\mathcal{F}^\Gamma$ to approximate velocity in the bulk and in the fracture network.

More precisely, we define the following discrete spaces for the velocities

$$
\begin{aligned}
&V^\Omega_h = \{v_f,\ f \in \mathcal{F}^\Omega\}\\
&V^\Omega_{h,g} = \{v_f \in V^\Omega_h : v_f = g_{\boldsymbol{u},f}\ \forall f \in \mathcal{F}^{\partial\Omega^u}\}\\
&V^\Omega_{h\,0} = \{v_f \in V^\Omega_h : v_f = 0\,\forall f \in \mathcal{F}^{\partial\Omega^u}\}\\
&V^\Gamma_h = \{\hat{v}_{\hat{f}},\ \hat{f} \in \mathcal{F}^\Gamma, : \textstyle\sum_{\hat{f}\in F} \hat{v}_{\hat{f}}\alpha_{\hat{c}(\hat{f}),\hat{f}} = 0,\ \forall F \in \mathcal{F}^\#_\Gamma\}\\
&V^\Gamma_{h,g} = \{v_{\hat{f}} \in V^\Gamma_h : v_{\hat{f}} = \hat{g}_{\hat{\boldsymbol{u}},\hat{f}}\,\forall \hat{f} \in \mathcal{F}^{I^u},\ v_{\hat{f}} = 0\,\forall \hat{f} \in \mathcal{F}^{I^F}\}\\
&V^\Gamma_{h\,0} = \{v_{\hat{f}} \in V^\Gamma_h : v_{\hat{f}} = 0\,\forall \hat{f} \in \mathcal{F}^{I^u},\ v_{\hat{f}} = 0\,\forall \hat{f} \in \mathcal{F}^{I^F}\}
\end{aligned}
\tag{37}
$$

where $g_{\boldsymbol{u},f} \in \mathbb{R}$ and $\hat{g}_{\hat{\boldsymbol{u}},\hat{f}} \in \mathbb{R}$ are approximation of the velocity boundary data, as detailed later on. Note that for the velocity in the bulk the degrees of freedom represent the average normal velocity on the faces, while in the fracure we consider the average velocity normal to the faces integrated across the fracture aperture. For the

pressure in the bulk and in the fracture, we have

$$M_h^\Omega = \{v_c,\ c \in \mathcal{C}^\Omega\},\ \text{and}\ M_h^\Gamma = \{v_{\hat{c}},\ \hat{c} \in \mathcal{C}^\Gamma\}. \tag{38}$$

Remark 3.1. *The condition $\sum_{\hat{f}\in F} \hat{v}_{\hat{f}}\alpha_{\hat{c}(\hat{f}),\hat{f}} = 0$ enforces the balance of fluxes at the intersections, and has been introduced in an essential way in the definition of the discrete space for velocity in the fracture network. However, its implementation in practice is cumbersome and in the numerical code the balance of fluxes has been implemented by a Lagrange multiplier technique, which in fact approximates the value of pressure at the intersection. Moreover, the use of Lagrange multipliers may allow to implement more general coupling conditions among fractures, like the one proposed in [26].*

We introduce the following global discrete spaces

$$\boldsymbol{W}_h = V_h^\Omega \times V_h^\Gamma \text{ and } \boldsymbol{M}_h = M_h^\Omega \times M_h^\Gamma, \tag{39}$$

and the corresponding $\boldsymbol{W}_{h0}$ and $\boldsymbol{W}_{hg}$. The jump and average of discrete bulk velocity across the fracture are defined as

$$[\![v_h]\!]_h = ([\![v_h]\!]_{\hat{c}}, \hat{c} \in \mathcal{C}^\Gamma), \quad \{v_h\}_h = (\{v_h\}_{\hat{c}}, \hat{c} \in \mathcal{C}^\Gamma)$$

where, because of the chosen convention about orientation, we have

$$[\![v_h]\!]_{\hat{c}} = v_{f^+(\hat{c})} - v_{f^-(\hat{c})} \quad \text{and} \quad \{v_h\}_{\hat{c}} = \frac{1}{2}\left(v_{f^+(\hat{c})} + v_{f^-(\hat{c})}\right).$$

We equip the given discrete spaces for velocity with the following norms,

$$\|v_h\|^2_{V_h^\Omega} = \sum_{c\in\mathcal{C}^\Omega} |c| \sum_{f\in\partial c} v_f^2 + \sum_{\hat{c}\in\mathcal{C}^\Gamma} |\hat{c}| \left([\![v_h]\!]^2_{\hat{c}} + \{v_h\}^2_{\hat{c}}\right), \quad \|\hat{v}_h\|^2_{V_h^\Gamma} = \sum_{\hat{c}\in\mathcal{C}^\Gamma} |\hat{c}| \sum_{\hat{f}\in\partial\hat{c}} \hat{v}_{\hat{f}}^2, \tag{40}$$

and

$$\|(v_h, \hat{v}_h)\|^2_{\boldsymbol{W}_h} = \|v_h\|^2_{V_h^\Omega} + \|\hat{v}_h\|^2_{V_h^\Gamma}. \tag{41}$$

Note that we have "strengthened" the norm on V_h^Ω by adding the contribution of the jump and average of velocity across the fracture to the standard definition. This choice is motivated by the analogy with the continuous case and is convenient for the following analysis. The standard choice would indeed be [22]

$$|||v_h|||^2_{V_h^\Omega} = \sum_{c\in\mathcal{C}^\Omega} |||v_h|||^2_c = \sum_{c\in\mathcal{C}^\Omega} |c| \sum_{f\in\partial c} v_f^2, \tag{42}$$

where with the c suffix we have indicated the norm operating on the velocity degrees of freedom of cell c However, we have the following

Lemma 3.1. *The discrete norms $|||\cdot|||_{V_h^\Omega}$ and $\|\cdot\|_{V_h^\Omega}$ are equivalent. More precisely,*

$$|||v_h|||_{V_h^\Omega} \le \|v_h\|_{V_h^\Omega} \le \sqrt{1 + \frac{C}{h}}\,|||v_h|||_{V_h^\Omega} \quad \forall v_h \in V_h^\Omega, \tag{43}$$

for a $C > 0$.

Proof. Evidently, $|||v_h|||_{V_h^\Omega} \le \|v_h\|_{V_h^\Omega}$. Because of the stated property of the polygonal mesh we have that there exists a $C > 0$ such that $|\hat{c}| \le Ch^{-1}|c^+(\hat{c})|$ and $|\hat{c}| \le Ch^{-1}|c^-(\hat{c})|$, for all $\hat{c} \in \mathcal{C}^\Gamma$. Moreover $[\![v_h]\!]^2_{\hat{c}} + \{v_h\}^2_{\hat{c}} \le 2(v^2_{f^+(\hat{c})} + v^2_{f^-(\hat{c})})$. Thus, there exists a $C > 0$ so that $(1 + \frac{C}{h})|||v_h|||^2_{V_h^\Omega} \ge \|v_h\|^2_{V_h^\Omega}$. □

For the spaces for pressure we have,

$$\|q_h\|^2_{M_h^\Omega} = \sum_{c\in\mathcal{C}^\Omega} |c| q_c^2, \quad \|\hat{q}_h\|^2_{M_h^\Gamma} = \sum_{\hat{c}\in\mathcal{C}^\Gamma} |\hat{c}| \hat{q}_{\hat{c}}^2, \tag{44}$$

and

$$\|(q_h, \hat{q}_h)\|^2_{\boldsymbol{M}_h} = \|q_h\|^2_{M_h^\Omega} + \|\hat{q}_h\|^2_{M_h^\Gamma}. \tag{45}$$

As customary in mimetic finite differences we define projectors on the discrete spaces. For the pressure spaces we define $\Pi^{M_h^\Omega} : M^\Omega \to M_h^\Omega$ and $\Pi^{M_h^\Gamma} : M^\Gamma \to M_h^\Gamma$ as

$$\Pi^{M_h^\Omega} q = \{\frac{1}{|c|}\int_c q,\, c \in \mathcal{C}^\Omega\} \quad \text{and} \quad \Pi^{M_h^\Gamma} \hat{q} = \{\frac{1}{|\hat{c}|}\int_{\hat{c}} \hat{q},\, \hat{c} \in \mathcal{C}^\Gamma\}. \tag{46}$$

As for velocity, the projectors are defined on subspaces of V^Ω and V^Γ such that the normal component of the velocity is integrable on each mesh face for the bulk and the fracture, respectively. More precisely, we define

$$V_+^\Omega = \{\boldsymbol{v} \in V^\Omega :\, \boldsymbol{v} \in [L^s(\Omega)]^d\}, \quad V_+^\Gamma = \{\hat{\boldsymbol{v}} \in V^\Gamma :\, \hat{\boldsymbol{v}} \in [L^s(\Gamma)]^{d-1}\} \tag{47}$$

for $s > 2$. We define then $\Pi^{V_h^\Omega} : V_+^\Omega \to V_h^\Omega$ and $\Pi^{V_h^\Gamma} : V_+^\Gamma \to V_h^\Gamma$ as

$$\begin{aligned} \Pi^{V_h^\Omega} \boldsymbol{v} &= \{\Pi_f^{V_h^\Omega} \boldsymbol{v},\, f \in \mathcal{F}^\Omega\} = \{\frac{1}{|f|}\int_f \boldsymbol{v}\cdot\boldsymbol{n}_f,\, f \in \mathcal{F}^\Omega\}, \\ \Pi^{V_h^\Gamma} \hat{\boldsymbol{v}} &= \{\Pi_{\hat{f}}^{V_h^\Gamma} \hat{\boldsymbol{v}} =,\, \hat{f} \in \mathcal{F}^\Gamma\} = \{\frac{1}{|\hat{f}|}\int_{\hat{f}} \hat{\boldsymbol{v}}\cdot\boldsymbol{n}_{\hat{f}},\, \hat{f} \in \mathcal{F}^\Gamma\}, \end{aligned} \tag{48}$$

where $\Pi_f^{V_h^\Omega}$ and $\Pi_{\hat{f}}^{V_h^\Gamma}$ are the local projectors on the degree of freedom of face f and $\hat{f}$, respectively.

Note that in the 2-dimensional case the fracture is one-dimensional so the fracture mesh faces reduce to points, and

$$\Pi^{V_h^\Gamma} \hat{\boldsymbol{v}} = \{\hat{\boldsymbol{v}}(\hat{f})\cdot\boldsymbol{n}_{\hat{f}},\, \hat{f} \in \mathcal{F}^\Gamma\},$$

which is well defined since in 1D elements of V^Γ have a continuous representative on each fracture γ_k. We will also use the notation

$$\boldsymbol{\Pi}^{\boldsymbol{M}_h} = \Pi^{M_h^\Omega} \times \Pi^{M_h^\Gamma} \quad \text{and} \quad \boldsymbol{\Pi}^{\boldsymbol{W}_h} = \Pi^{V_h^\Omega} \times \Pi^{V_h^\Gamma}.$$

.

The definition of the projectors allows us to better specify the terms $g_{\boldsymbol{u},f}$ and $\hat{g}_{\hat{\boldsymbol{u}},\hat{f}}$ in (37) as the face projection of the corresponding continuous terms, namely

$$g_{\boldsymbol{u},f} = \frac{1}{|f|}\int_f g_{\boldsymbol{u}} \quad \text{and} \quad \hat{g}_{\hat{\boldsymbol{u}},\hat{f}} = \frac{1}{|\hat{f}|}\int_{\hat{f}} \hat{g}_{\hat{\boldsymbol{u}}}.$$

3.3. Mimetic inner products in $\boldsymbol{M}_h$ and $\boldsymbol{W}_h$

Since $\boldsymbol{M}_h$ and $\boldsymbol{W}_h$ are product spaces it is convenient to separate the contribution of the bulk to that of the fracture. For M_h^Ω and M_h^Γ, the inner products are simply

$$(p_h, q_h)_{M_h^\Omega} = \sum_{c\in\mathcal{C}^\Omega} |c| p_c q_c \quad \text{and} \quad (\hat{p}_h, \hat{q}_h)_{M_h^\Gamma} = \sum_{\hat{c}\in\mathcal{C}^\Gamma} |\hat{c}| \hat{p}_{\hat{c}} \hat{q}_{\hat{c}} \tag{49}$$

and we set

$$\big((p_h, \hat{p}_h), (q_h, \hat{q}_h)\big)_{\boldsymbol{M}_h} = (p_h, q_h)_{M_h^\Omega} + (\hat{p}_h, \hat{q}_h)_{M_h^\Gamma}.$$

The inner products may be written in matrix form, by identifying the matrices $\mathrm{M}^{M_h^\Omega}$, $\mathrm{M}^{M_h^\Gamma}$ and $\mathrm{M}^{\boldsymbol{M}_h}$, as follows

$$\big((p_h,\hat{p}_h),(q_h,\hat{q}_h)\big)_{\boldsymbol{M}_h} = p_h^T,\mathrm{M}^{M_h^\Omega} q_h + \hat{p}_h^T \mathrm{M}^{M_h^\Gamma}\hat{q}_h = (p_h,\hat{p}_h)^T \mathrm{M}^{\boldsymbol{M}_h}(q_h,\hat{q}_h).$$

The matrices can be assembled by summing the contributions coming from each bulk and fracture cell, as standard in mimetic finite difference schemes. It can be noted that the space $\boldsymbol{M}_h$ and $\boldsymbol{W}_h$ are already endowed with scalar products that induce the norms introduced in (45) and (41), respectively.

Yet, for the discrete velocity space we need to construct a different inner product, called mimetic inner product, $A_h\big((u_h,\hat{u}_h),(v_h,\hat{v}_h)\big)$, which is in fact the discrete counterpart of the form $A\big((\boldsymbol{u},\hat{\boldsymbol{u}}),(\boldsymbol{v},\boldsymbol{v})\big)$ in (12). The presence of the coupling terms makes the structure of the mimetic inner product more complex than in the usual mimetic setting. Let $\mathrm{M}^{V_h^\Omega}$ and $\mathrm{M}^{V_h^\Gamma}$ be two standard MFD matrices that defines the mimetic inner product on $\mathcal{C}^\Omega$ and $\mathcal{C}^\Gamma$, respectively. They are built by cell-wise contributions,

$$\mathrm{M}^{V_h^\Omega} = \sum_c \mathrm{M}_c^{V_h^\Omega} \quad \text{and} \quad \mathrm{M}^{V_h^\Gamma} = \sum_{\hat{c}} \mathrm{M}_{\hat{c}}^{V_h^\Gamma},$$

whose expression will be detailed later on. In our case we have an additional contribution due to the presence of the fractures. Let C^Γ be the matrix for the coupling term expressed as

$$\mathrm{C}^\Gamma = \sum_{\hat{c}\in\mathcal{C}^\Gamma} \mathrm{C}_{\hat{c}}^\Gamma,$$

where the cell contribution $\mathrm{C}_{\hat{c}}^\Gamma$ is such that

$$w_h^T \mathrm{C}_{\hat{c}}^\Gamma v_h = \eta_{\hat{c}}|\hat{c}|(\{v_h\}_{\hat{c}}\{w_h\}_{\hat{c}} + \xi_0 [\![v_h]\!]_{\hat{c}}[\![w_h]\!]_{\hat{c}}).$$

The mimetic inner product for the discrete velocity space is then defined for any $(v_h,\hat{v}_h)$ and $(w_h,\hat{w}_h)$ in $\boldsymbol{W}_h$ as

$$A_h\big((v_h,\hat{v}_h),(w_h,\hat{w}_h)\big) = a_h(v_h,w_h)_{V_h^\Omega} + \hat{a}_h(\hat{v}_h,\hat{w}_h), \tag{50}$$

where

$$a_h(v_h,w_h) = m_h(v_h.w_h) + c_h(v_h,w_h) = v_h^T \mathrm{M}^{V_h^\Omega} w_h + v_h^T \mathrm{C}^\Gamma w_h = v_h^T \mathrm{A}^{V_h^\Omega} w_h, \tag{51}$$

and

$$\hat{a}_h(\hat{v}_h,\hat{w}_h) = \hat{v}_h^T \mathrm{M}^{V_h^\Omega} \hat{w}_h.$$

Here,

$$m_h(v_h.w_h) = v_h^T \mathrm{M}^{V_h^\Omega} w_h, \quad c_h(v_h,w_h) = v_h^T \mathrm{C}^\Gamma w_h, \tag{52}$$

and, clearly, $\mathrm{A}^{V_h^\Omega} = \mathrm{M}^{V_h^\Omega} + \mathrm{C}^\Gamma$. The choice of $\mathrm{M}^{V_h^\Omega}$ and $\mathrm{M}^{V_h^\Gamma}$ cannot be arbitrary. The corresponding $A_h\big((u_h,\hat{u}_h),(v_h,\hat{v}_h)\big)$ must satisfy some stability and consistency properties. Yet, we prefer to describe first our discrete problem in a general way and leave the description of the actual construction of the mimetic matrices and their properties to Section 3.6.

3.4. **Discrete divergence**

Formulation (12) allows us to identify a global divergence operator $\mathrm{DIV} : \boldsymbol{W} \to \boldsymbol{M}$ as follows

$$\mathrm{DIV}(\boldsymbol{v},\hat{\boldsymbol{v}}) = (\operatorname{div}\boldsymbol{v}, \operatorname{div}_{\boldsymbol{\tau}}\hat{\boldsymbol{v}} - [\![\boldsymbol{v}\cdot\boldsymbol{n}_\Gamma]\!]), \tag{53}$$

such that

$$B\big((\boldsymbol{v},\hat{\boldsymbol{v}}),(q,\hat{q})\big) = -\big(\mathrm{DIV}(\boldsymbol{v},\hat{\boldsymbol{v}}),(q,\hat{q})\big)_{\boldsymbol{M}}.$$

We now define its discrete counterpart $\mathrm{DIV}_h : \boldsymbol{W}_h \to \boldsymbol{M}_h$ as

$$\mathrm{DIV}_h(v_h, \hat{v}_h) = (\mathrm{div}_h\, v_h, \mathrm{div}_{\boldsymbol{\tau},h}\, \hat{v}_h - [\![v_h]\!]_h), \tag{54}$$

where

$$\mathrm{div}_h\, v_h = (\frac{1}{|c|}\sum_{f\in\partial c} |f| v_f \alpha_{c,f},\ c\in\mathcal{C}^\Omega), \quad \mathrm{div}_{\boldsymbol{\tau},h}\, \hat{v}_h = (\frac{1}{|\hat{c}|}\sum_{\hat{f}\in\partial\hat{c}} \hat{|}\hat{f}| v_{\hat{f}} \alpha_{\hat{c},\hat{f}},\ \hat{c}\in\mathcal{C}^\Gamma), \tag{55}$$

We will approximate the term $B\big((\boldsymbol{v},\hat{\boldsymbol{v}}),(q,\hat{q})\big)$ with

$$B_h\big((v_h,\hat{v}_h),(q_h,\hat{q}_h)\big) = -\big(\mathrm{DIV}_h(v_h,\hat{v}_h),(q_h,\hat{q}_h)\big)_{\boldsymbol{M}_h}. \tag{56}$$

Lemma 3.2. *The divergence and projection operators commute. i.e.* $\mathrm{DIV}_h\, \boldsymbol{\Pi}^{\boldsymbol{W}_h}(\boldsymbol{v},\hat{\boldsymbol{v}}) = \boldsymbol{\Pi}^{\boldsymbol{M}_h}\mathrm{DIV}(\boldsymbol{v},\hat{\boldsymbol{v}})$.

Proof. The existence of the following commuting diagrams

$$\begin{array}{ccc} V^\Omega & \xrightarrow{\mathrm{div}} & M^\Omega \\ \downarrow{\scriptstyle \Pi^{V_h^\Omega}} & & \downarrow{\scriptstyle \Pi^{M_h^\Omega}} \\ V_h^\Omega & \xrightarrow{\mathrm{div}_h} & M_h^\Omega \end{array} \quad \text{and} \quad \begin{array}{ccc} V^\Gamma & \xrightarrow{\mathrm{div}_{\boldsymbol{\tau}}} & M^\Gamma \\ \downarrow{\scriptstyle \Pi^{V_h^\Gamma}} & & \downarrow{\scriptstyle \Pi^{M_h^\Gamma}} \\ V_h^\Gamma & \xrightarrow{\mathrm{div}_{\boldsymbol{\tau},h}} & M_h^\Gamma \end{array}$$

is a standard result of mimetic finite differences, see [22]. Moreover,

$$[\![\Pi^{V_h^\Omega}\boldsymbol{v}]\!]_{\hat{c}} = \left(\frac{1}{|f^+(\hat{c})|}\int_{f^+(\hat{c})} \boldsymbol{v}^+\cdot\boldsymbol{n}_{f^+(\hat{c})} - \frac{1}{|f^-(\hat{c})|}\int_{f^-(\hat{c})}\boldsymbol{v}^-\cdot\boldsymbol{n}_{f^-(\hat{c})}\right) = \frac{1}{|\hat{c}|}\int_{\hat{c}}[\![\boldsymbol{v}\cdot\boldsymbol{n}_\Gamma]\!] = \Pi_{\hat{c}}^{M_h^\Gamma}[\![\boldsymbol{v}\cdot\boldsymbol{n}_\Gamma]\!],$$

since $|f^+(\hat{c})| = |f^-(\hat{c})| = |\hat{c}|$ and $\boldsymbol{n}_{f^+(\hat{c})} = -\boldsymbol{n}_{f^-(\hat{c})} = \boldsymbol{n}_\Gamma$ by construction. □

3.5. **The discrete problem**

The discrete problem is: *Find* $(u_h,\hat{u}_h)\in\boldsymbol{W}_{hg}$ *and* $(p_h,\hat{p}_h)\in\boldsymbol{M}_h$ *so that*

$$\begin{cases} A_h\big((u_h,\hat{u}_h),(v_h,\hat{v}_h)\big) + B_h\big((v_h,\hat{v}_h,(p_h,\hat{p}_h)\big) = F_h^u\big((v_h,\hat{v}_h)\big), \\ B_h\big((u_h,\hat{u}_h),(q_h,\hat{q}_h)\big) = F_h^p\big((q_h,\hat{q}_h)\big), \end{cases} \tag{57}$$

for all $(v_h,\hat{v}_h)\in\boldsymbol{W}_{h0}$ *and* $(q_h,\hat{q}_h)\in\boldsymbol{M}_h$. Here, F_h^u and F_h^p are functionals that account for the forcing and boundary terms, namely

$$F_h^u\big((v_h,\hat{v}_h)\big) = -\sum_{f\in\mathcal{F}^{\partial\Omega p}} v_f\int_f g_P - \sum_{\hat{f}\in\mathcal{F}^{Ip}} v_{\hat{f}}\int_{\hat{f}} g_{\hat{p}}, \tag{58}$$

$$F_h^p\big((q_h,\hat{q}_h)\big) = -\sum_{c\in\mathcal{C}^\Omega} q_c\int_c f - \sum_{\hat{c}\in\mathcal{C}^\Gamma}\hat{q}_{\hat{c}}\int_{\hat{c}}\hat{f}. \tag{59}$$

3.6. **Construction and properties of inner product operators**

We will construct the elemental matrices $\mathrm{M}_c^{V_h^\Omega}$ and $\mathrm{M}_{\hat{c}}^{V_h^\Gamma}$ using the standard procedure for mimetic finite differences that we recall for completeness.

Let $\boldsymbol{x}_\beta$ with $\beta = c, \hat{c}, f, \hat{f}$ indicate the baricenter of the respective entity. For each c and $\hat{c}$ we define the matrices

$$\mathrm{N}_c = \begin{bmatrix} \boldsymbol{n}_{f_1}^T \\ \vdots \\ \boldsymbol{n}_{f_{N_c^\partial}}^T \end{bmatrix} \boldsymbol{K}_c \quad \text{and} \quad \mathrm{N}_{\hat{c}} = \begin{bmatrix} \boldsymbol{n}_{\hat{f}_1}^T \\ \vdots \\ \boldsymbol{n}_{\hat{f}_{N_{\hat{c}}^\partial}}^T \end{bmatrix} \hat{\boldsymbol{K}}_c,$$

where $\{f_1, \dots, f_{N_c^\partial}\}$ and $\{\hat{f}_1, \dots, \hat{f}_{N_{\hat{c}}^\partial}\}$ denote the faces at the boundary of c and $\hat{c}$ respectively. While,

$$\mathrm{R}_c = \begin{bmatrix} \alpha_{c,f_1}|f_1|(\boldsymbol{x}_{f_1} - \boldsymbol{x}_c)^T \\ \vdots \\ \alpha_{c,f_{N_c^\partial}}|f_{N_c^\partial}|(\boldsymbol{x}_{f_{N_c^\partial}} - \boldsymbol{x}_c)^T \end{bmatrix} \quad \text{and} \quad \mathrm{R}_{\hat{c}} = \begin{bmatrix} |\alpha_{\hat{c},\hat{f}_{N_{\hat{c}}^\partial}}|\hat{f}_1|(\boldsymbol{x}_{\hat{f}_1} - \boldsymbol{x}_{\hat{c}})^T \\ \vdots \\ \alpha_{\hat{c},\hat{f}_{N_{\hat{c}}^\partial}}|\hat{f}_{N_{\hat{c}}^\partial}|(\boldsymbol{x}_{f_{N_{\hat{c}}^\partial}} - \boldsymbol{x}_{\hat{c}})^T \end{bmatrix}.$$

Then, we set

$$\mathrm{M}_c^{V_h^\Omega} = \mathrm{R}_c(\mathrm{R}_c^T\mathrm{N}_c)^{-1}\mathrm{R}^T + \frac{\mathrm{tr}(\mathrm{R}_c\boldsymbol{K}_c^{-1}\mathrm{R}_c^T)}{|c|N_c^\partial}(\mathrm{I}_c - \mathrm{N}_c(\mathrm{N}_c^T\mathrm{N}_c)^{-1}\mathrm{N}_c^T), \tag{60}$$

$$\mathrm{M}_{\hat{c}}^{V_h^\Gamma} = \mathrm{R}_{\hat{c}}(\mathrm{R}_{\hat{c}}^T\mathrm{N}_{\hat{c}})^{-1}\mathrm{R}^T + \frac{\mathrm{tr}(\mathrm{R}_{\hat{c}}\hat{\boldsymbol{K}}_{\hat{c}}^{-1}\mathrm{R}_{\hat{c}}^T)}{|\hat{c}|N_{\hat{c}}^\partial}(\mathrm{I}_{\hat{c}} - \mathrm{N}_{\hat{c}}(\mathrm{N}_{\hat{c}}^T\mathrm{N}_{\hat{c}})^{-1}\mathrm{N}_{\hat{c}}^T). \tag{61}$$

This is not the only possible construction but it is a quite common one and it allows us to state the following lemma

Lemma 3.3. *Thank to hypothesis A1 and A2 made on the bulk and fracture mesh, we have that*

$$\frac{1}{K_c^*}|c|\sum_{f\in\partial c}|v_f|^2 \lesssim v_h^T\mathrm{M}_c^{V_h^\Omega}v_h \lesssim \frac{1}{K_{c,*}}|c|\sum_{f\in\partial c}|v_f|^2 \tag{62}$$

and

$$\frac{1}{\hat{\boldsymbol{K}}_{\hat{c}}^*}|\hat{c}|\sum_{\hat{f}\in\partial\hat{c}}|v_{\hat{f}}|^2 \lesssim \hat{v}_h^T\mathrm{M}_{\hat{c}}^{V_h^\Gamma}\hat{v}_h \lesssim \frac{1}{\hat{\boldsymbol{K}}_{\hat{c},*}}|\hat{c}|\sum_{\hat{f}\in\partial\hat{c}}|v_{\hat{f}}|^2, \tag{63}$$

where the local matrix-vector products involve only the degrees of freedom on ∂c and $\partial\hat{c}$, respectively. As a consequence,

$$\frac{1}{K^*}|||v_h|||_{V_h^\Omega}^2 \lesssim m_h(v_h, v_h) \lesssim \frac{1}{K_*}|||v_h|||_{V_h^\Omega}^2 \tag{64}$$

and

$$\frac{1}{\hat{K}^*}\|\hat{v}_h\|_{V_h^\Gamma}^2 \lesssim \hat{a}_h(\hat{v}_h, \hat{v}_h) \lesssim \frac{1}{\hat{K}_*}\|\hat{v}_h\|_{V_h^\Gamma}^2. \tag{65}$$

Proof. The proof is a standard result of mimetic inner products defined with the given matrices. We omit the details that may be found, for instance, in [20, 22]. □

This result is sufficient to prove stability for the mimetic norm for the discrete velocity space in the fracture. For the bulk, however, we have to handle the coupling terms properly. We have the following

Lemma 3.4. *For $\xi_0 > 0$ the form $a_h(\cdot,\cdot)$ is stable with respect to the $\|\cdot\|_{V_h^\Omega}$ norm. More precisely,*

$$\min(K^{*-1}, \eta_*\min(1,\xi_0))\|v_h\|_{V_h^\Omega}^2 \lesssim a_h(v_h, v_h) \lesssim \max(K_*^{-1}, \eta^*\max(1,\xi_0))\|v_h\|_{V_h^\Omega}^2, \quad \forall v_h \in V_h^\Omega. \tag{66}$$

Moreover, $A_h(\cdot,\cdot)$ is stable with respect to the $\|\cdot\|_{\boldsymbol{W}_h}$ norm: $\forall (v_h,\hat{v}_h)\in \boldsymbol{W}_h$ we have

$$\zeta_*\|(v_h,\hat{v}_h)\|^2_{\boldsymbol{W}_h} \lesssim A_h\big((v_h,\hat{v}_h),(v_h,\hat{v}_h)\big) \lesssim \zeta^*\|(v_h,\hat{v}_h)\|^2_{\boldsymbol{W}_h}, \tag{67}$$

where

$$\zeta_* = \min\big(\hat{K}^{*-1}, K^{*-1}, \eta_*\min(1,\xi_0)\big), \text{ and } \zeta^* = \max\big(\hat{K}_*^{-1}, K_*^{-1}, \eta^*\max(1,\xi_0)\big). \tag{68}$$

Proof. Since $c_h(v_h,v_h) = \sum_{\hat{c}\in\mathcal{C}^\Gamma}|\hat{c}|\eta_{\hat{c}}\{v_h\}^2_{\hat{c}} + \xi_0\sum_{\hat{c}\in\mathcal{C}^\Gamma}|\hat{c}|\eta_{\hat{c}}[\![v_h]\!]^2_{\hat{c}}$, we deduce that

$$\min(1,\xi_0)\eta_*\sum_{\hat{c}\in\mathcal{C}^\Gamma}|\hat{c}|\left(\{v_h\}^2_{\hat{c}} + [\![v_h]\!]^2_{\hat{c}}\right) \le c_h(v_h,v_h) \le \max(1,\xi_0)\eta^*\sum_{\hat{c}\in\mathcal{C}^\Gamma}|\hat{c}|\left(\{v_h\}^2_{\hat{c}} + [\![v_h]\!]^2_{\hat{c}}\right), \tag{69}$$

and (66) follows from (64) and the definition of a_h in (51). The bounds on A_h are then a consequence of the previous result, inequalities (65) and the definition of A_h in (50). □

3.6.1. *The case $\xi_0 = 0$*

We have already mentioned that the case $\xi_0 = 0$ is peculiar. Indeed, we will show in the following that the discrete problem allows to take $\xi_0 = 0$ and in the section devoted to numerical results we will show that for that value we indeed obtain $\{p_h\}_h = \hat{p}_h$, as expected. We have the following

Lemma 3.5. *There are two positive constants, here indicated by C_* and C, so that for any $h>0$ and*

$$0 \ge \xi_0 > -\frac{C_* h}{2K^*\eta^*(1+Ch)} \tag{70}$$

there is a $C_{\xi_0}(h)>0$ which depends on ξ_0, the mesh size (as well as the problem parameters) with $\lim_{h\to 0^+} C_{\xi_0}(h) = 0$ and such that

$$A_h\big((v_h,\hat{v}_h),(v_h,\hat{v}_h)\big) \ge C_{\xi_0}(h)\|(v_h,\hat{v}_h)\|^2_{\boldsymbol{W}_h}.$$

Consequently, A_h is stable also for $\xi_0 = 0$, for all $h>0$.

Proof. To extend the previous stability result we need only to examine the lower bound of (67) for the case $\xi_0 < 0$. Thanks to (43) we have that there exists a constant $C_*>0$ so that

$$m_h(v_h,v_h) \ge \frac{1}{2}\frac{C_*}{K^*}|||v_h|||^2_{V_h^\Omega} + \frac{C_* h}{2K^*(1+Ch)}\|v_h\|^2_{V_h^\Omega} \ge \frac{1}{2}\frac{C_*}{K^*}|||v_h|||^2_{V_h^\Omega} + \frac{C_* h}{2K^*(1+Ch)}\sum_{\hat{c}\in\mathcal{C}^\Gamma}|\hat{c}|(\{v_h\}^2_{\hat{c}} + [\![v_h]\!]^2_{\hat{c}}).$$

If $\xi_0 \le 0$ we have that $c_h(v_h,v_h) \ge \xi_0\eta^*\sum_{\hat{c}\in\mathcal{C}^\Gamma}|\hat{c}|\left(\{v_h\}^2_{\hat{c}} + [\![v_h]\!]^2_{\hat{c}}\right)$, and thus

$$a_h(v_h,v_h) \ge \frac{1}{2}\frac{C_*}{K^*}|||v_h|||^2_{V_h^\Omega} + \Big(\frac{C_* h}{2K^*(1+Ch)} + \xi_0\eta^*\Big)\sum_{\hat{c}\in\mathcal{C}^\Gamma}|\hat{c}(|\{v_h\}^2_{\hat{c}} + [\![v_h]\!]^2_{\hat{c}}),$$

which allows us to get a positive lower bound for a_h (and thus A_h) if $\frac{C_* h}{2K^*(1+Ch)} + \xi_0\eta^* > 0$, that is if $\xi_0 > -\frac{C_* h}{2K^*\eta^*(1+Ch)}$. The upper bound for A_h remains that of (67). □

3.7. **Consistency of A_h**

Because of the coupling terms we need to consider a more general definition of consistency than the standard one used for instance in [22]. Let first define some spaces and state some known facts for readers' convenience.

For some $s > 2$, for all $c \in \mathcal{C}^\Omega$ and for all $\hat{c} \in \mathcal{C}^\Gamma$ let us consider the local cell-based spaces

$$S_c^\Omega = \{\boldsymbol{v}_c \in [L^s(c)]^d,\, \mathrm{div}\, \boldsymbol{v}_c = \mathrm{const},\, \boldsymbol{v}_c \cdot \boldsymbol{n}_f = \mathrm{const}, \forall f \in \partial c\},$$

and

$$S_{\hat{c}}^\Gamma = \{\hat{\boldsymbol{v}}_{\hat{c}} \in [L^s(\hat{c})]^{d-1},\, \mathrm{div}\, \hat{\boldsymbol{v}}_{\hat{c}} = \mathrm{const},\, \hat{\boldsymbol{v}}_{\hat{c}} \cdot \boldsymbol{n}_{\hat{f}} = \mathrm{const}, \forall \hat{f} \in \partial c\}.$$

Remark 3.2. *The condition $s > 2$ is a technical requirement needed to guarantee the stability of the projection operator. However, in the 2D case $s = 2$ is sufficient for the velocity space in the fracture cells.*

We also define the following cell-based test spaces

$$\tau_c^\Omega = \{\boldsymbol{v}_c^\tau = \boldsymbol{K}_c \nabla q_c,\, q_c \in \mathbb{P}^1(c)\} \quad \text{and} \quad \tau_{\hat{c}}^\Gamma = \{\hat{\boldsymbol{v}}_{\hat{c}}^\tau = \hat{\boldsymbol{K}}_{\hat{c}} \nabla_{\boldsymbol{\tau}}\, \hat{q}_{\hat{c}},\, \hat{q}_{\hat{c}} \in \mathbb{P}^1(\hat{c})\},$$

It is immediate to verify that $\tau_c^\Omega \subset S_c^\Omega$. $\tau_{\hat{c}}^\Gamma \subset S_{\hat{c}}^\Gamma$ We also define the following global spaces:

$$\begin{aligned} S_h^\Omega &= \{\boldsymbol{v} \in V^\Omega : \boldsymbol{v}|_c \in S_c^\Omega, \boldsymbol{v} \cdot \boldsymbol{n}_f = v_f,\, \forall c \in \mathcal{C}^\Omega,\, \forall f \in \mathcal{F}^\Omega\}, \\ S_h^\Gamma &= \{\hat{\boldsymbol{v}} \in V^\Gamma : \hat{\boldsymbol{v}}|_{\hat{c}} \in S_{\hat{c}}^\Gamma,\, \hat{\boldsymbol{v}} \cdot \boldsymbol{n}_{\hat{f}} = \hat{v}_{\hat{f}},\, \forall \hat{c} \in \mathcal{C}^\Gamma,\, \forall \hat{f} \in \mathcal{F}^\Gamma\}, \end{aligned} \tag{71}$$

where v_f and $\hat{v}_{\hat{f}}$ are constant values taken on the mesh faces. While,

$$\tau_h^\Omega = \{\boldsymbol{v}^\tau \in L^2(\Omega_\Gamma) :\, \boldsymbol{v}^\tau|_c \in \tau_c^\Omega\} \quad \text{and } \tau_h^\Gamma = \{\hat{\boldsymbol{v}}^\tau \in L^2(\Gamma) :\, \hat{\boldsymbol{v}}^\tau|_{\hat{c}} \in \tau_{\hat{c}}^\Omega\}. \tag{72}$$

We also define the global product spaces

$$S_h = S_h^\Omega \times S_h^\Gamma \quad \text{and} \quad \tau_h = \tau_h^\Omega \times \tau_h^\Gamma. \tag{73}$$

The projection operators $\Pi^{V_h^\Omega}$ and $\Pi^{V_h^\Gamma}$ are surjective from S_h^Ω to V_h^Ω and from S_h^Γ to V_h^Γ, respectively.

Because of the coupling terms the consistency conditions cannot be written just cell-wise as usual in the analysis of mimetic schemes. So we first note that the form A is well defined on the space $L \times [L^2(\Gamma)]^{d-1} \supset \boldsymbol{W}$, where $L = \{\boldsymbol{v} \in L^2(\Omega) : \boldsymbol{v} \cdot \boldsymbol{n}_\Gamma \in [L^2(\Gamma)]^{d-1}\}$. We can also trivially extend A_h to a broken discrete velocity space $\tilde{\boldsymbol{W}}_h$ where the degrees of freedom on the internal faces are duplicated to account for the (possibly different) values in each cell. Analogously we could extend the velocity projection operators from τ_h onto $\tilde{\boldsymbol{W}}_h$, by computing the projections cell-wise.

However, to avoid making the notation heavier we will in the following use the symbols A_h, $\boldsymbol{\Pi}^{\boldsymbol{W}_h}$ etc. to indicate also their extended counterparts, since the context will not leave ambiguity on that respect.

Lemma 3.6. *We have the following consistency conditions.*

- *Local consistency conditions. For all $c \in \mathcal{C}^\Omega$, $\hat{c} \in \mathcal{C}^\Gamma$ and for all $(\boldsymbol{v}^\tau, \hat{\boldsymbol{v}}^\tau) \in \tau_c^\Omega \times \tau_{\hat{c}}^\Gamma$ and $(\boldsymbol{w}, \hat{\boldsymbol{w}}) \in S_c^\Omega \times S_{\hat{c}}^\Gamma$ we have*

$$m_{h,c}(\Pi_c^{V_h^\Omega} \boldsymbol{v}^\tau, \Pi_c^{V_h^\Omega} \boldsymbol{w}) = \int_c \nabla q_c \cdot \boldsymbol{w}, \quad \hat{a}_{\hat{c}}(\Pi_{\hat{c}}^{V_h^\Gamma} \hat{\boldsymbol{v}}^\tau, \Pi_{\hat{c}}^{V_h^\Omega} \hat{\boldsymbol{w}}) = \int_{\hat{c}} \nabla_{\boldsymbol{\tau}}\, \hat{q}_{\hat{c}} \cdot \hat{\boldsymbol{w}}, \tag{74}$$

  where $m_{h,c}$ and $\hat{a}_{\hat{c}}$ denotes restriction to the corresponding cell degrees of freedom of the forms m_h and a_h defined in (51) and (52).
- *Global consistency condition. For all $(\boldsymbol{v}^\tau, \hat{\boldsymbol{v}}^\tau) \in \tau_h$ and for all $(\boldsymbol{w}, \hat{\boldsymbol{w}}) \in S_h$ we have*

$$A_h\big((\Pi^{V_h^\Omega} \boldsymbol{v}^\tau, \Pi^{V_h^\Gamma} \hat{\boldsymbol{v}}^\tau), (\Pi^{V_h^\Omega} \boldsymbol{w}, \Pi^{V_h^\Gamma} \hat{\boldsymbol{w}})\big) = A\big((\boldsymbol{v}^\tau, \hat{\boldsymbol{v}}^\tau), (\boldsymbol{w}, \hat{\boldsymbol{w}})\big) = \sum_{c \in \mathcal{C}^\Omega} \int_c \nabla q \cdot \boldsymbol{w} + \sum_{\hat{c} \in \mathcal{C}^\Gamma} \int_{\hat{c}} \nabla_{\boldsymbol{\tau}}\, \hat{q} \cdot \hat{\boldsymbol{w}} + c(\boldsymbol{v}^\tau, \boldsymbol{w}) \tag{75}$$

Proof. The local consistency conditions are standard results because of the given choice of mimetic matrices. The global consistency is obtained by summing the local contributions and by noting that

$$c_h(\Pi^{V_h^\Omega}\boldsymbol{w},\Pi^{V_h^\Omega}\boldsymbol{v}^\tau)=\sum_{\hat{c}\in\mathcal{C}^\Gamma}\eta_{\hat{c}}|\hat{c}|(\{\Pi^{V_h^\Omega}\boldsymbol{w}\}_{\hat{c}}\{\Pi^{V_h^\Omega}\boldsymbol{v}^\tau\}_{\hat{c}}+\xi_0[\![\Pi^{V_h^\Omega}\boldsymbol{w}]\!]_{\hat{c}}[\![\Pi^{V_h^\Omega}\boldsymbol{v}^\tau]\!]_{\hat{c}})= \tag{76}$$

$$\int_\Gamma\eta\left(\{\boldsymbol{w}\cdot\boldsymbol{n}_\Gamma\}\{\boldsymbol{v}^\tau\cdot\boldsymbol{n}_\Gamma\}+\xi_0[\![\boldsymbol{w}\cdot\boldsymbol{n}_\Gamma]\!][\![\boldsymbol{v}^\tau\cdot\boldsymbol{n}_\Gamma]\!]\right)=c(\boldsymbol{w},\boldsymbol{v}^\tau). \tag{77}$$

We have exploited the fact that η is (by hypothesis) piecewise constant, while functions in S_h^Ω and τ_h^Ω have constant normal components on cell faces, and thus constant average and jump on each fracture cell. □

We also have the following

Corollary 3.1. *For all $(\boldsymbol{v}^\tau,\hat{\boldsymbol{v}}^\tau)\in\tau_h$ and for all $(\boldsymbol{w},\hat{\boldsymbol{w}})\in S_h$ we have*

$$A_h((\Pi^{V_h^\Omega}\boldsymbol{v}^\tau,\Pi^{V_h^\Gamma}\hat{\boldsymbol{v}}^\tau),(\Pi^{V_h^\Omega}\boldsymbol{w},\Pi^{V_h^\Gamma}\hat{\boldsymbol{w}}))=-\int_{\Omega_\Gamma}q\,\mathrm{div}\,\boldsymbol{w}-\int_\Gamma\hat{q}\mathrm{div}_{\boldsymbol{\tau}}\,\boldsymbol{w}+$$
$$\sum_{c\in\mathcal{C}^\Omega}\sum_{f\in\partial c}\alpha_{c,f}w_f^I\int_f q+\sum_{\hat{c}\in\mathcal{C}^\Gamma}\sum_{\hat{f}\in\partial\hat{c}}\alpha_{\hat{c},\hat{f}}\hat{w}_{\hat{f}}^I\int_{\hat{f}}\hat{q}+c(\boldsymbol{v}^\tau,\boldsymbol{w}).$$

where $w_f^I=\boldsymbol{w}\cdot\boldsymbol{n}_f$ and $\hat{w}_{\hat{f}}^I=\hat{\boldsymbol{w}}\cdot\boldsymbol{n}_{\hat{f}}$ indicate the constant normal components on the respective faces.

Consequently, by setting $(q^I,\hat{q}^I)=\boldsymbol{\Pi}^{\boldsymbol{M}_h}(q,\hat{q})$, we have that

$$A_h((\Pi^{V_h^\Omega}\boldsymbol{v}^\tau,\Pi^{V_h^\Gamma}\hat{\boldsymbol{v}}^\tau),(w_h,\hat{w}_h))=-(\mathrm{div}_h\,w_h,q^I)_{M_h^\Omega}-(\mathrm{div}_{\tau,h}\,\hat{w}_h,\hat{q}^I)_{M_h^\Gamma}+$$
$$\sum_{c\in\mathcal{C}^\Omega}\sum_{f\in\partial c}\alpha_{c,f}w_f\int_f q+\sum_{\hat{c}\in\mathcal{C}^\Gamma}\sum_{\hat{f}\in\partial\hat{c}}\alpha_{\hat{c},\hat{f}}\hat{w}_{\hat{f}}\int_{\hat{f}}\hat{q}+c_h(\Pi^{V_h^\Omega}\boldsymbol{v}^\tau,w_h), \tag{78}$$

for any $(w_h,\hat{w}_h)\in\boldsymbol{W}_h$.

Proof. This result is an extension of a classical result for mimetic finite differences, which may be found in the cited references, and is obtained by integrating by parts the terms in (75) and treating the terms on the fracture cells separately. □

Corollary 3.2. *Let $(\boldsymbol{u},\hat{\boldsymbol{u}})$ and $(p,\hat{p})$ be solution of (12). Let furthermore assume that $(p,\hat{p})\in H^1(\Omega_\Gamma)\times H^1(\Gamma)$. Let us take $(\boldsymbol{v}^\tau,\hat{\boldsymbol{v}}^\tau)\in\tau_h$, $(q^I,\hat{q}^I)=\Pi^{M_h^\Omega}q\times\Pi^{M_h^\Gamma}\hat{q}$, where q and $\hat{q}$ are the functions defining elements of τ^h, and $(u_h^I,\hat{u}_h^I)=\Pi^{V_h^\Omega}(\boldsymbol{u},\hat{\boldsymbol{u}})$. We further set $(v_h^\tau,\hat{v}_h^\tau)=\boldsymbol{\Pi}^{\boldsymbol{W}_h}(\boldsymbol{v}^\tau,\hat{\boldsymbol{v}}^\tau)$. Then,*

$$c(\boldsymbol{u},\boldsymbol{v}^\tau)=c_h(u_h^I,\Pi^{V_h^\Omega}\boldsymbol{v}^\tau)=\sum_{\hat{c}\in\mathcal{C}^\Gamma}\int_{\hat{c}}(\{p\}_{\hat{c}}-\hat{p})[\![\boldsymbol{v}^\tau\cdot\boldsymbol{n}_\Gamma]\!]_{\hat{c}}+\int_{\hat{c}}[\![p]\!]_{\hat{c}}\{\boldsymbol{v}^\tau\cdot\boldsymbol{n}_\Gamma\}_{\hat{c}}. \tag{79}$$

Proof. The first equality in (79) is obtained by noting that in the derivation of (76) it is not necessary that $\boldsymbol{w}\in S_h^\Omega$, but it is sufficient that $\boldsymbol{w}\in V^\Omega$. So I can use (76) with $\boldsymbol{w}=\boldsymbol{u}$ and obtain the desided result.

Thanks to the regularity assumptions on p and $\hat{p}$ we can counter-integrate by parts the terms in the first equation in (12), and deduce by standard means that for any $\boldsymbol{v}\in\boldsymbol{W}_0$

$$c(\boldsymbol{u},\boldsymbol{v})=\int_\Gamma[\![p\boldsymbol{v}\cdot\boldsymbol{n}_\Gamma]\!]-\int_\Gamma\hat{p}[\![\boldsymbol{v}\cdot\boldsymbol{n}_\Gamma]\!]=\int_\Gamma(\{p\}-\hat{p})[\![\boldsymbol{v}\cdot\boldsymbol{n}_\Gamma]\!]+\int_\Gamma[\![p]\!]\{\boldsymbol{v}\cdot\boldsymbol{n}_\Gamma\}, \tag{80}$$

which effectively enforces the coupling conditions. We now note that $\boldsymbol{v}^\tau\cdot\boldsymbol{n}_\Gamma$ is piecewise constant on Γ and thus in $L^2(\Gamma)$. As a consequence, there is a $\boldsymbol{w}\in V_0^\Omega$ so that $\boldsymbol{w}\cdot\boldsymbol{n}_\Gamma=\boldsymbol{v}^\tau\cdot\boldsymbol{n}_\Gamma$ on Γ. If we set $\boldsymbol{v}=\boldsymbol{w}$ in (80) we easily obtain the second equality in (79). □

3.8. **Inf-sup condition for the discrete spaces**

We state the following Lemma.

Lemma 3.7. *The form $B_h : \boldsymbol{W}_h \times \boldsymbol{M}_h \to \mathbb{R}$ defined in (56) is inf-sup stable.*

Proof. The inf-sup stability for B_h derives directly from the commuting property expressed in Lemma 3.2. Given a $(q_h, \hat{q}_h) \in \boldsymbol{M}_h$ we construct problems (21), (24) and (32) with $(q, \hat{q}) \in \boldsymbol{M}$ taken such that $q|_c = q_c$ and $\hat{q}|_{\hat{c}} = \hat{q}_{\hat{c}}$, for all cells in the bulk and the fractures. We indicate with $(\boldsymbol{v}, \hat{\boldsymbol{v}}) \in \boldsymbol{W}$ the corresponding velocities. We recall that $\boldsymbol{v} = \boldsymbol{v}_1 + \boldsymbol{v}_2$ where $\boldsymbol{v}_1$ is solution of (21), while $\boldsymbol{v}_2 = \prod_{\alpha=1}^{N_\alpha} \boldsymbol{v}_\alpha$, each $\boldsymbol{v}_\alpha$ being the gradient of the solution of (32).

We set $(v_h, \hat{v}_h) = (\Pi^{V_h^\Gamma} \boldsymbol{v}, \Pi^{V_h^\Gamma} \hat{\boldsymbol{v}})$, $v_1 = \Pi^{V_h^\Gamma} \boldsymbol{v}_1$, $v_2 = \Pi^{V_h^\Gamma} \boldsymbol{v}_2$ (clearly $v_h = v_1 + v_2$). By construction, $[\![\boldsymbol{v} \cdot \boldsymbol{n}_\Gamma]\!]$ is constant on each fracture γ_k and thus is constant on each cell $\hat{c} \in \mathcal{C}^\Gamma$, consequently $\Pi_{\hat{c}}^{M_h^\Gamma}([\![\boldsymbol{v} \cdot \boldsymbol{n}_\Gamma]\!]) = [\![v_h]\!]_{\hat{c}}$ and $|\hat{c}|[\![v_h]\!]_{\hat{c}} = \int_{\hat{c}} [\![\boldsymbol{v} \cdot \boldsymbol{n}_\Gamma]\!]$. Therefore, by using the commuting property of projectors,

$$
\begin{aligned}
B_h\big((v_h, \hat{v}_h), (q_h, \hat{q}_h)\big) = -\big(\mathrm{DIV}_h(v_h, \hat{v}_h), (q_h, \hat{q}_h)\big)_{\boldsymbol{M}_h} = -\big(\boldsymbol{\Pi}^{\boldsymbol{M}_h} \mathrm{DIV}(\boldsymbol{v}, \hat{\boldsymbol{v}}), (q_h, \hat{q}_h)\big)_{\boldsymbol{M}_h} = \\
- \sum_{c \in \mathcal{C}^\Omega} q_c \int_c \operatorname{div} \boldsymbol{v}_1 - \sum_{\hat{c} \in \mathcal{C}^\Gamma} \hat{q}_{\hat{c}} \left(\int_{\hat{c}} \operatorname{div}_\tau \hat{\boldsymbol{v}} \, d\Gamma - |\hat{c}| [\![v_h]\!]_{\hat{c}} \right) = - \int_{\Omega_\Gamma} q \operatorname{div} \boldsymbol{v} - \int_\Gamma \hat{q} \left(\operatorname{div}_\tau \hat{\boldsymbol{v}} - [\![\boldsymbol{v} \cdot \boldsymbol{n}_\Gamma]\!] \right) d\Gamma = \\
= B\big((\boldsymbol{v}, \hat{\boldsymbol{v}}), (q, \hat{q})\big) = \|(q_h, \hat{q}_h))\|^2_{\boldsymbol{M}_h},
\end{aligned}
$$

where we have exploited the fact that $\|(q, \hat{q})\|_{\boldsymbol{M}} = \|(q_h, \hat{q}_h)\|_{\boldsymbol{M}_h}$.

We now recall (without giving the proof) some known results about mimetic projectors. We assume some extra regularity on $\hat{\boldsymbol{v}}$ and the $\boldsymbol{v}_\alpha$ (we have already assumed that $\boldsymbol{v}_1 \in H^1(\Omega)$), and in particular that $\hat{\boldsymbol{v}} \in V_+^\Gamma$ and $\boldsymbol{v}_\alpha \in L^s(\Omega_\alpha)$ for a $s > 2$. This is sufficient to derive that

$$
\|\hat{v}_h\|_{V_h^\Gamma} \lesssim \|\hat{q}_h\|_{M_h^\Gamma}, \quad |||v_1|||_{V_h^\Omega} \lesssim \|q_h\|_{M_h^\Omega} \quad \text{and} \quad |||v_2|||_{V_h^\Omega} \lesssim \|q_h\|_{M_h^\Omega},
$$

see, for instance, [19, 22]. Therefore, we are left to show that

$$
\sum_{\hat{c} \in \mathcal{C}^\Gamma} |\hat{c}| \left([\![v_2]\!]^2_{\hat{c}} + \{v_2\}^2_{\hat{c}} \right) + \sum_{\hat{c} \in \mathcal{C}^\Gamma} |\hat{c}| \{v_1\}^2_{\hat{c}} \lesssim \|q_h\|^2_{M_h^\Omega},
$$

where we used the fact that $[\![v_1]\!] = 0$ by construction. Indeed, by using the properties of the flux carriers and trace inequalities,

$$
\begin{aligned}
&\textstyle\sum_{\hat{c} \in \mathcal{C}^\Gamma} |\hat{c}| \left([\![v_2]\!]^2_{\hat{c}} + \{v_2\}^2_{\hat{c}} \right) = \sum_k \sum_{\hat{c} \in \mathcal{C}^\Gamma{}_k} |\hat{c}| \left([\![z_k]\!]^2 + \{z_k\}^2 \right) \lesssim \|q\|^2_{L^2(\Omega)} = \|q_h\|^2_{M_h^\Omega}, \\
&\textstyle\sum_{\hat{c} \in \mathcal{C}^\Gamma} |\hat{c}| \{v_1\}^2_{\hat{c}} \lesssim \sum_{\hat{c} \in \mathcal{C}^\Gamma} \|\boldsymbol{v}_1 \cdot \boldsymbol{n}_\Gamma\|^2_{L^2(\hat{c})} \lesssim \|\boldsymbol{v}_1\|^2_{H^1(\Omega)} \lesssim \|q\|^2_{L^2(\Omega)} = \|q_h\|^2_{M_h^\Omega}.
\end{aligned}
$$

We can then conclude that $\|(v_h, \hat{v}_h)\|_{\boldsymbol{W}_h} \lesssim \|(q, \hat{q})\|_{\boldsymbol{M}_h}$ and, consequently, B_h is inf-sup stable. □

3.9. **Convergence Results**

In this section we give a convergence result of our mimetic discretization. To this purpose, we recall some known results.

Let $\mathcal{P}$ be a polyedron in $\mathbb{R}^d$ for $d = 2$ or $d = 3$ of diameter h_P.

Lemma 3.8. *For any function $q \in H^2(\mathcal{P})$ there exists a linear polynomial $q^1_{\mathcal{P}} \in \mathbb{P}^1(\mathcal{P})$ such that*

$$
\|q - q^1_{\mathcal{P}}\|_{L^2(\mathcal{P})} + h_{\mathcal{P}} \|\nabla(q - q^1_{\mathcal{P}})\|_{L^2(\mathcal{P})} \lesssim h^2_{\mathcal{P}} |q|_{H^2(\mathcal{P})}.
$$

Lemma 3.9. *For every $q \in H^1(\mathcal{P})$*

$$\sum_{f\in\partial\mathcal{P}} \|q\|^2_{L^2(f)} \lesssim h_{\mathcal{P}}^{-1}\|q\|^2_{L^2(\mathcal{P})} + h_{\mathcal{P}}|\nabla q|^2_{L^2(\mathcal{P})}.$$

As a consequence, it may be shown that (see for instance [19]) that under the same hypothesis of Lemma 3.8,

$$\|q - q^1_{\mathcal{P}}\|^2_{L^2(f)} + h^2_{\mathcal{P}}\|\nabla(q - q^1_{\mathcal{P}})\|^2_{L^2(f)} \lesssim h^3_{\mathcal{P}}|q|_{H^2(\mathcal{P})},\ \forall f \in \partial\mathcal{P}. \tag{81}$$

The previous Lemmas are direct consequence of standard results of approximation and mimetic finite difference theory, see [22, Lemmas 5.1 and 5.2] [19, Lemma 5.2] and [18, Lemma 4.3.8], and their proof is not reported here.

Lemma 3.10. *Let $(q, \hat{q}) \in H^2(\Omega_\Gamma) \times H^2(\Gamma)$ and $(q^1, \hat{q}^1)$ piecewise linear polynomials so that q^1_c and $\hat{q}^1_{\hat{c}}$ satisfy the assumptions of Lemma 3.8. Then, for any $(v_h, \hat{v}_h) \in \boldsymbol{W}_h$ we have that*

$$|m_h\big(\Pi^{V^\Omega_h}(\boldsymbol{K}\nabla(q - q^1)\big), v_h)\big)| + |\hat{a}_h\big(\Pi^{V^\Gamma_h}(\hat{\boldsymbol{K}}\nabla_{\boldsymbol{\tau}}(\hat{q} - \hat{q}^1)), \hat{v}_h\big)| \lesssim \Upsilon h|(q, \hat{q})|_{H^2(\Omega_\Gamma)\times H^2(\Gamma)}\|(v_h, \hat{v}_h)\|_{\boldsymbol{W}_h}, \tag{82}$$

where $\Upsilon = \max\big(\max_c \frac{K^*_c}{K_{c,*}}, \max_{\hat{c}} \frac{K^*_{\hat{c}}}{K_{\hat{c},*}}\big)$.

Proof. We first consider a single cell $c \in \mathcal{C}^\Omega$ and we set $g_h = \Pi^{V^\Omega_h}\boldsymbol{K}\nabla(q - q^1)$. We indicate with $m_c(g_h, v_h)$ the restriction of m_h to the given cell. Thanks to Cauchy-Schwarz inequality and (62)

$$\big(m_c(g_h, v_h)\big)^2 \le m_c(g_h, g_h)m_c(v_h, v_h) \lesssim (K_{c,*})^{-1}|c| \sum_{f\in\partial c} |g_f|^2\, m_c(v_h, v_h).$$

By definition of the projector and (81),

$$|g_f|^2 = \frac{1}{|f|^2}\left(\int_f \boldsymbol{K}\nabla(q - q^1)\right)^2 \le \frac{(K^*_c)^2}{|f|}\|\nabla(q - q^1)\|^2_{L^2(f)} \lesssim h_c\frac{(K^*_c)^2}{|f|}|q|^2_{H^2(c)}.$$

Since $|c|/|f| \lesssim h_c$, we have

$$m_c(g_h, g_h) \lesssim h^2_c\frac{(K^*_c)^2}{K_{c,*}}|q|^2_{H^2(f)}.$$

Using again (62) to bound $m_c(v_h, v_h)$, summing over all elements, and finally taking the square root we have

$$|m_h\big(\Pi^{V^\Omega_h}(\boldsymbol{K}\nabla(q - q^1)\big), v_h)\big)| \lesssim \max_c \frac{K^*_c}{K_{c,*}}h|q|_{H^2(\Omega_\Gamma)}\|v_h\|_{V^\Omega_h}.$$

We can repeat the same process for $\hat{a}_h\big(\Pi^{V^\Gamma_h}(\hat{\boldsymbol{K}}\nabla_{\boldsymbol{\tau}}(\hat{q} - \hat{q}^1)), \hat{v}_h\big)$ to obtain $|\hat{a}_h\big(\Pi^{V^\Gamma_h}(\hat{\boldsymbol{K}}\nabla_{\boldsymbol{\tau}}(\hat{q} - \hat{q}^1)), \hat{v}_h\big)| \lesssim \max_{\hat{c}} \frac{K^*_{\hat{c}}}{K_{\hat{c},*}}h|\hat{q}|^2_{H^2(\Gamma)}\|\hat{v}_h\|_{V^\Gamma_h}$, by which we get the final result. □

Remark 3.3. *We recall that in the following we consider homogeneous velocity flux conditions at the boundary of the fracture network, which includes fully immersed fractures, we have assumed $I^p = \emptyset$. However, the following convergence result can be generalized to the case of pressure imposed on part of the boundary of the fracture network, as well as to the case of coefficients that vary within the elements, by making some additional hypotheses on their regularity and following the techniques illustrated in [21, 22].*

Theorem 3.1. *Let $U = (\boldsymbol{u}, \hat{\boldsymbol{u}}) \in \boldsymbol{W}$ and $P = (p, \hat{p}) \in \boldsymbol{M}$ be solution of problem (12). Let assume that $P \in H^2(\Omega_\Gamma) \times H^2(\Gamma)$. Then, the numerical solution $U_h = (u_h, \hat{u}_h) \in \boldsymbol{W}_h$ of (57) satisfies*

$$\|(\boldsymbol{u}, \hat{\boldsymbol{u}}) - \boldsymbol{\Pi}^{\boldsymbol{W}_h}(\boldsymbol{u}, \hat{\boldsymbol{u}})\|_{\boldsymbol{W}_h} \lesssim \frac{\Upsilon}{\zeta_*} h \|(p, \hat{p})\|_{H^2(\Omega_\Gamma)\times H^2(\Gamma)}, \tag{83}$$

where Υ and ζ_* have been defined in Lemma 3.10 and in (68), respectively, and the hidden constant does depend neither on the problem parameters nor on h.

Proof. To simplify the notation we set $U_h^I = \boldsymbol{\Pi}^{\boldsymbol{W}_h}\boldsymbol{U}$, and $E_h = (e_h, \hat{e}_h) = U_h^I - U_h$ and $P = (p, \hat{p})$. While, $P_h = (p_h, \hat{p}_h)$ is solution of (57). Moreover, we indicate with $P^1 = (p^1, \hat{p}^1) \in \boldsymbol{M}$ the piecewise discontinuous linear approximation of P whose restriction on each cell satisfy Lemma 3.8, and we set

$$V^\tau = \{(\boldsymbol{v}^\tau, \hat{\boldsymbol{v}}^\tau) : \boldsymbol{v}_c^\tau = -\boldsymbol{K}\nabla p^1|_c,\, \hat{\boldsymbol{v}}_{\hat{c}}^\tau = -\hat{\boldsymbol{K}}\nabla_{\boldsymbol{\tau}}\, \hat{p}^1|_{\hat{c}}\}, \tag{84}$$

while $(v_h^\tau, \hat{v}_h^\tau) = V_h^\tau = \boldsymbol{\Pi}^{\boldsymbol{W}_h} V^\tau$. The stability of A_h stated in Lemma 3.4 allows us to write that

$$\zeta_* \|U_h - U_h^I\|_{\boldsymbol{W}_h}^2 = \zeta_* \|E_h\|_{\boldsymbol{W}_h}^2 \lesssim A_h(E_h, E_h) = A_h(U_h, E_h) - A_h(U_h^I, E_h).$$

Using the fact the U_h is our discrete solution and that $B_h(E_h, P_h) = 0$, we have

$$A_h(U_h, E_h) = -B_h(E_h, P_h) + F_h^u(E_h) = F_h^u(E_h),$$

while

$$A_h(U_h^I, E_h) = A_h(U_h^I - V_h^\tau, E_h) + A_h(V_h^\tau, E_h).$$

Thanks to (78), we may write

$$\begin{aligned}
-A_h(V_h^\tau, E_h) = &-(\mathrm{div}_h\, e_h, p_h^1)_{M_h^\Omega} - (\mathrm{div}_{\tau,h}\, \hat{e}_h, \hat{p}_h^1)_{M_h^\Gamma} + \\
&\sum_{c\in\mathcal{C}^\Omega}\sum_{f\in\partial c} \alpha_{c,f} e_f \int_f p^1 + \sum_{\hat{c}\in\mathcal{C}^\Gamma}\sum_{\hat{f}\in\partial\hat{c}} \alpha_{\hat{c},\hat{f}}\hat{e}_{\hat{f}} \int_{\hat{f}} \hat{p}^1 - c_h(v_h^\tau, e_h) = \\
B_h(E_h, P_h^1) + &\sum_{c\in\mathcal{C}^\Omega}\sum_{f\in\partial c} \alpha_{c,f} e_f \int_f p^1 + \sum_{\hat{c}\in\mathcal{C}^\Gamma}\sum_{\hat{f}\in\partial\hat{c}} \alpha_{\hat{c},\hat{f}}\hat{e}_{\hat{f}} + [\![e]\!]_{\hat{f}} \int_{\hat{c}} \hat{p}^1 - \sum_{\hat{c}\in\mathcal{C}^\Gamma} [\![e]\!]_{\hat{c}} \int_{\hat{c}} \hat{p}^1 - c_h(v_h^\tau, e_h) = \\
&\sum_{c\in\mathcal{C}^\Omega}\sum_{f\in\partial c} \alpha_{c,f} e_f \int_f p^1 + \sum_{\hat{c}\in\mathcal{C}^\Gamma}\sum_{\hat{f}\in\partial\hat{c}} \alpha_{\hat{c},\hat{f}}\hat{e}_{\hat{f}} \int_{\hat{c}} \hat{p}^1 - \sum_{\hat{c}\in\mathcal{C}^\Gamma} [\![e]\!]_{\hat{c}} \int_{\hat{c}} \hat{p}^1 - c_h(v_h^\tau, e_h),
\end{aligned}$$

since $B_h(E_h, P_h^1) = 0$. Moreover, since $e_h \in V_{h\,0}^\Omega$, and pressures $(p, \hat{p})$ are continuous across internal bulk and fracture mesh faces, respectively, we get

$$\begin{aligned}
&\sum_{c\in\mathcal{C}^\Omega}\sum_{f\in\partial c} \alpha_{c,f} e_f \int_f p^1 = \sum_{\hat{c}\in\mathcal{C}^\Gamma} [\![e_h \int_{\hat{c}} p^1]\!]_{\hat{c}} + \sum_{c\in\mathcal{C}^\Omega}\sum_{f\in\partial c\setminus\Gamma} \alpha_{c,f} e_f \int_f p^1 = \\
&\sum_{\hat{c}\in\mathcal{C}^\Gamma} [\![e_h \int_{\hat{c}} p^1]\!]_{\hat{c}} + \sum_{f\in\mathcal{F}_I^\Omega} e_f [\![\int_f p^1]\!]_f + \sum_{f\in\mathcal{F}^{\partial\Omega p}} e_f \int_f p^1 = \sum_{\hat{c}\in\mathcal{C}^\Gamma} [\![e_h \int_{\hat{c}} p^1]\!]_{\hat{c}} + \sum_{f\in\mathcal{F}_I^\Omega} e_f [\![\int_f (p^1 - p)]\!]_f + \sum_{f\in\mathcal{F}^{\partial\Omega p}} e_f \int_f p^1.
\end{aligned}$$

And, since we are treating here the case $I^p = \emptyset$,

$$\sum_{\hat{c}\in\mathcal{C}^\Gamma}\sum_{\hat{f}\in\partial\hat{c}}\alpha_{\hat{c},\hat{f}}\hat{e}_{\hat{f}}\int_{\hat{f}}\hat{p}^1 = \sum_{\hat{f}\in\mathcal{F}_I^\Gamma}\hat{e}_{\hat{f}}[\![\int_{\hat{f}}\hat{p}^1]\!]_{\hat{f}} + \sum_{F\in\mathcal{F}_\Gamma^\#}\sum_{\hat{f}\in F}\alpha_{\hat{c}(\hat{f}),\hat{f}}\hat{e}_{\hat{f}}\int_{\hat{f}}\hat{p}^1, =$$
$$\sum_{\hat{f}\in\mathcal{F}_I^\Gamma}\hat{e}_{\hat{f}}[\![\int_{\hat{f}}(\hat{p}^1-\hat{p})]\!]_{\hat{f}} + \sum_{F\in\mathcal{F}_\Gamma^\#}\sum_{\hat{f}\in F}\alpha_{\hat{c}(\hat{f}),\hat{f}}\hat{e}_{\hat{f}}\int_{\hat{f}}(\hat{p}^1-\hat{p}),$$

where we have also exploited the fact that $\sum_{F\in\mathcal{F}_\Gamma^\#}\sum_{\hat{f}\in F}\alpha_{\hat{f},\hat{c}(\hat{f})}\hat{e}_{\hat{f}} = 0$ because of the coupling condition at the interface.

We now note that, thanks to Eq. (79),

$$c_h(v_h^\tau, e_h) = c_h(v_h^\tau - u_h^I, e_h) + c_h(u_h^I, e_h) = c_h(v_h^\tau - u_h^I, e_h) + \sum_{\hat{c}\in\mathcal{C}^\Gamma}([\![e_h\int_{\hat{c}}p]\!]_{\hat{c}} - [\![e_h]\!]_{\hat{c}}\int_{\hat{c}}\hat{p}).$$

Therefore, using the definition of $F_h^u(E_h)$, collecting and rearranging all previous results, we obtain

$$\|E_h\|^2_{\boldsymbol{W}_h} = \|U_h - U_h^I\|^2_{\boldsymbol{W}_h} \lesssim -A_h(U_h^I - V_h^\tau, E_h) + c_h(u_h^I - v_h^\tau, e_h) + \sum_{\hat{c}\in\mathcal{C}^\Gamma}[\![e_h\int_{\hat{c}}(p^1-p)]\!]_{\hat{c}} + \sum_{f\in\mathcal{F}_I^\Omega}e_f[\![\int_f(p^1-p)]\!]_f +$$
$$\sum_{f\in\mathcal{F}^{\partial\Omega_P}}e_f\int_f(p-p^1) + \sum_{\hat{f}\in\mathcal{F}_I^\Gamma}\hat{e}_{\hat{f}}[\![\int_{\hat{f}}(\hat{p}^1-\hat{p})]\!]_{\hat{f}} + \sum_{F\in\mathcal{F}_\Gamma^\#}\sum_{\hat{f}\in F}\alpha_{\hat{f},\hat{c}(\hat{f})}\hat{e}_{\hat{f}}\int_{\hat{f}}(\hat{p}-\hat{p}^1).$$

We have that

$$-A_h(U_h^I - V_h^\tau, E_h) + c_h(u_h^I - v_h^\tau, e_h) = m_h\big(\Pi^{V_h^\Omega}(\boldsymbol{K}\nabla(p-p^1)), e_h)\big) + \hat{a}_h\big(\Pi^{V_h^\Gamma}(\hat{\boldsymbol{K}}\nabla_{\boldsymbol{\tau}}(\hat{p}-\hat{p}^1)), \hat{e}_h)\big),$$

and we can use Lemma 3.10. All other terms are upper bounded by a term proportional to $h\|E_h\|_{\boldsymbol{W}_h}|P|_{H^2(\Omega_\Gamma)\times H^2(\Gamma)}$, thanks to the application of Cauchy-Schwartz inequality and of Lemmas 3.8, 3.9 and 3.10. For instance,

$$\sum_{\hat{c}\in\mathcal{C}^\Gamma}[\![e_h\int_{\hat{c}}(p^1-p)]\!]_{\hat{c}} = \sum_{\hat{c}\in\mathcal{C}^\Gamma}[\![e_h]\!]_{\hat{c}}\int_{\hat{c}}\{p^1-p\} + \{e_h\}_{\hat{c}}\int_{\hat{c}}[\![p^1-p]\!] \lesssim$$
$$\sqrt{\sum_{\hat{c}\in\mathcal{C}^\Gamma}|\hat{c}|\,([\![e_h]\!]^2_{\hat{c}} + \{e_h\}^2_{\hat{c}})}\sqrt{\sum_{\hat{c}\in\mathcal{C}^\Gamma}\int_{\hat{c}}\{p^1-p\}^2 + [\![p^1-p]\!]^2} \le \|E_h\|_{\boldsymbol{W}_h}\sqrt{\sum_{\hat{c}\in\mathcal{C}^\Gamma}\int_{\hat{c}}\{p^1-p\}^2 + [\![p^1-p]\!]^2}.$$

Now, since $\hat{c}$ is a boundary face of two bulk cells, I can use Lemma 3.9 to bound the integral over fracture cells with bulk cell integrals, and the use Lemma 3.8 to get the wanted result.

We give now the details for the term $\sum_{f\in\mathcal{F}_I^\Omega}e_f[\![\int_f(p^1-p)]\!]_f$. We have,

$$\left|\sum_{f\in\mathcal{F}_I^\Omega}e_f[\![\int_f(p^1-p)]\!]_f\right| \le \sqrt{\sum_{c\in\mathcal{C}^\Omega}|c|\sum_{f\in\partial c}e_f^2}\sqrt{\sum_{c\in\mathcal{C}^\Omega}|c|^{-1}\sum_{f\in\partial c}\left(\int_f(p^1-p)\right)^2} \le$$
$$\|e_h\|_{V_h^\Omega}\sqrt{\sum_{c\in\mathcal{C}^\Omega}|c|^{-1}\sum_{f\in\partial c}\left(\int_f(p^1-p)\right)^2}.$$

Now, thanks to (36) we have $|f| \lesssim h_c^{-1}|c|$ for all $f \in \partial c$, thus

$$\sum_{c\in\mathcal{C}^\Omega} |c|^{-1} \sum_{f\in\partial c} \left(\int_f (p^1 - p)\right)^2 \lesssim \sum_{c\in\mathcal{C}^\Omega} h_c^{-1} \sum_{f\in\partial c} \|p^1 - p\|^2_{L^2(f)} \lesssim \sum_{c\in\mathcal{C}^\Omega} h_c^{-2} \left(\|p^1 - p\|^2_{L^2(c)} + h_c^2 \|\nabla p^1 - \nabla p\|^2_{L^2(c)}\right) \lesssim \sum_{c\in\mathcal{C}^\Omega} h_c^2 |p^1 - p|^2_{H^2(c)} \lesssim h^2 |P|^2_{H^2(\Omega_\Gamma)\times H^2(\Gamma)},$$

and, consequently,

$$\left| \sum_{f\in\mathcal{F}_I^\Omega} e_f [\![\int_f (p^1 - p)]\!]_f \right| \lesssim h \|e_h\|_{\boldsymbol{W}_h} |P|^2_{H^2(\Omega_\Gamma)\times H^2(\Gamma)}.$$

The other terms can be treated similarly and we are able to obtain the desired estimate for the error in velocity. □

Remark 3.4. *We may note that the constant of estimate* (83) *depends not only on the value of bulk permeability and the effective permeability in the fracture, but also on the level of "anisotropy" of the permeability tensors through* Υ.

Theorem 3.2. *Under the same hypotheses of Theorem 3.1, the solution* $P_h = (p_h, \hat{p}_h) \in \boldsymbol{M}_h$ *of* (57) *satisfies*

$$\|(p_h, \hat{p}_h) - \boldsymbol{\Pi}^{\boldsymbol{M}_h}(p, \hat{p})\|_{\boldsymbol{M}_h} \lesssim \frac{\Upsilon\zeta^*}{\beta\zeta_*} h \|(p, \hat{p})\|_{H^2(\Omega_\Gamma)\times H^2(\Gamma)}, \tag{85}$$

where Υ *and* ζ_* *have been defined in Lemma 3.10 and in* (68)*, respectively, while* β *is the constant in the inf-sup inequality of Lemma 2.3. The hidden constant does depend neither on the problem parameters nor on* h.

Proof. Given the result of the previous theorem, a possible proof is obtained by extending the steps illustrated in [22, Section 5.2.4] to our case. We follow another route which requires to assume the existence of a stable reconstruction operator for the velocity (see the cited reference for a general discussion of reconstruction operators in mimetic finite differences).

A stable reconstruction operator $\mathcal{R}^{\boldsymbol{W}} = \mathcal{R}^\Omega \times \mathcal{R}^\Gamma : \boldsymbol{W}_h \to S_h$ is such that $\boldsymbol{\Pi}^{\boldsymbol{W}_h} \circ \mathcal{R} = \mathcal{I}$, where $\mathcal{I}$ is the identity operator, and

$$\|\mathcal{R}^{\boldsymbol{W}}(v_h, \hat{v}_h)\|_{\boldsymbol{W}} \lesssim \|(v_h, \hat{v}_h)\|_{\boldsymbol{W}_h}, \quad \forall (v_h, \hat{v}_h) \in \boldsymbol{W}_h. \tag{86}$$

We recall that the space S_h has been defined in (71) and (73).

We also define $\mathcal{R}^P : (q_h, \hat{q}_h) \in \boldsymbol{M}_h \to (q, \hat{q}) = \mathcal{R}^P(q_h, \hat{q}_h) \in \boldsymbol{M}$ so that $q|_c = q_c$ and $\hat{q}|_{\hat{c}} = \hat{q}_{\hat{c}}$, for all cells in the bulk and the fracture. Obviously $\boldsymbol{\Pi}^{\boldsymbol{M}_h} \circ \mathcal{R}^P = \mathcal{I}$.

We use the same definitions of U, U_h, P, P_h, V^τ and P^1, while we set $P_h^I = (p_h^I, \hat{p}_h^I) = \boldsymbol{\Pi}^{\boldsymbol{M}_h}(p, \hat{p})$. We construct $V^P = (\boldsymbol{v}^P, \hat{\boldsymbol{v}}^P)$ as the velocities that satisfy (21), (24) and (32) with $(q, \hat{q}) = \mathcal{R}^P(P_h - P_h^I)$, which means that

$$B\big(V^P, \mathcal{R}^P(P_h - P_h^I)\big) = \|\mathcal{R}^P(P_h - P_h^I)\|^2_{L^2(\Omega_\Gamma)\times L^2(\Gamma)} = \|P_h - P_h^I\|^2_{\boldsymbol{M}_h}.$$

We then set $V_h^P(v_h^P, \hat{v}_h^P) = \boldsymbol{\Pi}^{\boldsymbol{W}_h} V^P$ and $S_h \ni V_{\mathcal{R}}^P = (\boldsymbol{v}_{\mathcal{R}}^P, \hat{\boldsymbol{v}}_{\mathcal{R}}^P) = \mathcal{R} V_h^P$. Clearly, $\boldsymbol{\Pi}^{\boldsymbol{W}_h} V_{\mathcal{R}}^P = V_h^P$, and, moreover, because of the definition of the projector and of S_h we have that for all $c \in \mathcal{C}^\Omega$ and $\hat{c} \in \mathcal{C}^\Gamma$

$$\int_c \operatorname{div} \boldsymbol{v}_{\mathcal{R}}^P = |c| \operatorname{div} \boldsymbol{v}_{\mathcal{R}}^P|_c = \int_c \operatorname{div} \boldsymbol{v}^P, \quad \int_{\hat{c}} \operatorname{div} \hat{\boldsymbol{v}}_{\mathcal{R}}^P = |\hat{c}| \operatorname{div}_{\boldsymbol{\tau}} \hat{\boldsymbol{v}}_{\mathcal{R}}^P|_{\hat{c}} = \int_{\hat{c}} \operatorname{div}_{\boldsymbol{\tau}} \hat{\boldsymbol{v}}^P \quad \text{and} \quad [\![\boldsymbol{v} \cdot \mathbf{n}_\Gamma {}^P \mathcal{R}]\!]_{\hat{c}} = [\![\boldsymbol{v} \cdot \mathbf{n}_\Gamma {}^P]\!]_{\hat{c}}. \tag{87}$$

By construction of V^P, and since $\mathcal{R}^p(P_h - P_h^I)$ is cell-wise constant, we have

$$B(V_{\mathcal{R}}^P, \mathcal{R}^P(P_h - P_h^I)) = -\big(\mathrm{DIV}\, V^P, \mathcal{R}^p(P_h - P_h^I)\big)_{\boldsymbol{M}} = -\sum_{c\in\mathcal{C}^\Omega}\int_c (p_c - p)\,\mathrm{div}\,\boldsymbol{v}^P - \sum_{\hat{c}\in\mathcal{C}^\Gamma}\int_{\hat{c}} (\hat{p}_c - \hat{p})(\mathrm{div}_{\boldsymbol{\tau}}\,\hat{\boldsymbol{v}}^P - [\![\boldsymbol{v}\cdot\mathbf{n}_\Gamma{}^P]\!]_{\hat{c}})$$

$$B(V^P, \mathcal{R}^p(p_h - p_h^I)) = \|P_h - P_h^I\|^2_{\boldsymbol{M}_h},$$

where, as usual, the pedices c and $\hat{c}$ indicate the corresponding cell values of p_h and $\hat{p}_h$, respectively.

Furthermore, the commuting property of the global divergence operators and the previous result, allows us to write

$$B_h(V_h^P, P_h - P_h^I) = -(\boldsymbol{\Pi}^{\boldsymbol{M}_h}\,\mathrm{DIV}\, V^P, P_h - P_h^I)_{\boldsymbol{M}_h} = B(V_{\mathcal{R}}^P, \mathcal{R}^P(P_h - P_h^I)) = \|P_h - P_h^I\|^2_{\boldsymbol{M}_h}.$$

We also have the following equality

$$B_h(V_h^P, P_h - P_h^I) = B_h(V_h^P, P_h) - B_h(V_h^P, P_h^I) = -B_h(V_h^P, P_h^I) - A_h(U_h, V_h^P) + F_h^u(V_h^P),$$

and, exploiting again the fact that P_h^I is piecewise constant and the definition of the interpolation operators, we deduce that

$$B_h(V_h^P, P_h^I) = B(V_{\mathcal{R}}^P, P) = -A(U, V_{\mathcal{R}}^P) + F^u(V_{\mathcal{R}}^P).$$

Since the normal component of $\boldsymbol{v}_{\mathcal{R}}^P$ are piecewise constant on the boundary of Ω_Γ, by the definition of F^u and F_h^u we infer that $F_h^u(V_h^P) - F^u(V_{\mathcal{R}}^P) = 0$ and, consequently

$$\|P_h - P_h^I\|^2_{\boldsymbol{M}_h} = B_h(V_h^P, P_h) - B_h(V_h^P, P_h^I) = A(U, V_{\mathcal{R}}^P) - A_h(U_h, V_h^P).$$

We now exploit the global consistency condition (75) with $(\Pi^{V_h^\Omega}\boldsymbol{v}^\tau, \Pi^{V_h^\Gamma}\hat{\boldsymbol{v}}^\tau) = V_h^\tau = \boldsymbol{\Pi}^{\boldsymbol{W}_h} V^\tau$ and $(\Pi^{V_h^\Omega}\boldsymbol{w}, \Pi^{V_h^\Gamma}\hat{\boldsymbol{w}}) = V_h^P$, where V^τ is defined in (84), to obtain

$$A_h(U_h, V_h^P) = A_h(U_h - V_h^\tau, V_h^P) + A_h(V_h^\tau, V_h^P) = A_h(U_h - V_h^\tau, V_h^P) + A(V^\tau, V_{\mathcal{R}}^P),$$

and thus, by the continuity of A_h and A

$$\|P_h - P_h^I\|^2_{\boldsymbol{M}_h} = A_h(V_h^\tau - U_h, V_h^P) + A(U - V^\tau, V_{\mathcal{R}}^P) \lesssim \zeta^*\|U_h - V_h^\tau\|_{\boldsymbol{W}_h}\|V_h^P\|_{\boldsymbol{W}_h} + \zeta^*\|U - V^\tau\|_{\boldsymbol{W}}\|V_{\mathcal{R}}^P\|_{\boldsymbol{W}}. \quad (88)$$

We now note that, by using Theorem 3.1 and Lemmas 3.8 and 3.9 and the definition of V^τ and V_h^τ, we can deduce that

$$\|U_h - V_h^\tau\|_{\boldsymbol{W}_h} \le \|E_h\|_{\boldsymbol{W}_h} + \|U_h^I - V_h^\tau\|_{\boldsymbol{W}_h} \lesssim \frac{\Upsilon}{\zeta_*} h\|(p,\hat{p})\|_{H^2(\Omega_\Gamma)\times H^2(\Gamma)},$$

while we also have $\|U - V^\tau\|_{\boldsymbol{W}} \lesssim \frac{1}{\zeta_*} h\|(p,\hat{p})\|_{H^2(\Omega_\Gamma)\times H^2(\Gamma)}$.

By construction of V_h^P and $V_{\mathcal{R}}^P$, as well as the stability of the reconstruction operator, we have

$$\|V_h^P\|_{\boldsymbol{W}_h} \lesssim \frac{1}{\beta}\|P_h - P_h^I\|_{\boldsymbol{M}_h} \quad \text{and} \quad \|V_{\mathcal{R}}^P\|_{\boldsymbol{W}} \lesssim \frac{1}{\beta}\|P_h - P_h^I\|_{\boldsymbol{M}_h}.$$

We can then obtain the desired result thanks to (88). □

Remark 3.5. *We will see in the section dedicated to numerical results that one can obtain a super-optimal convergence of the pressure. The study of super-convergence properties may be done following the techniques presented in [22], but is beyond the scope of this work.*

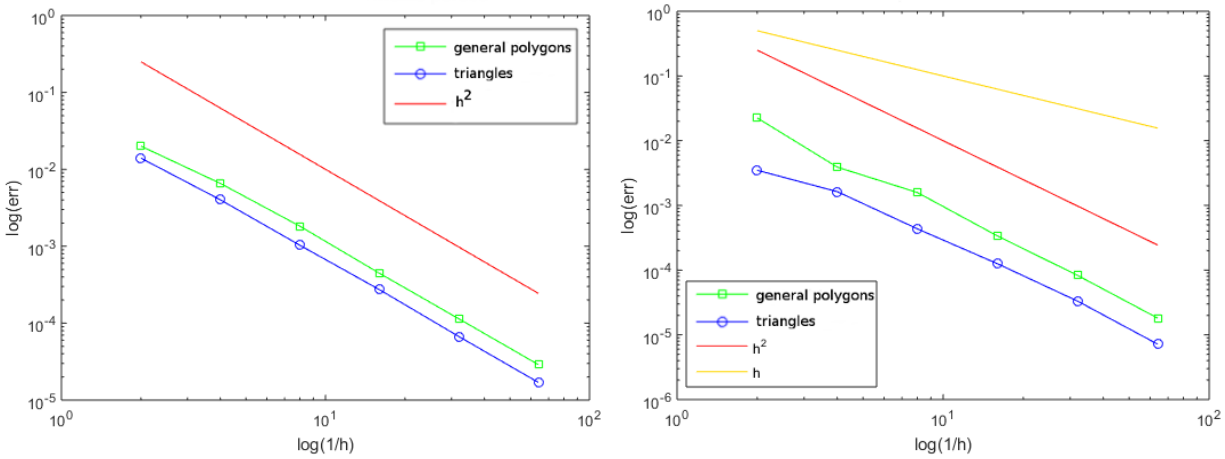

FIGURE 4. Relative error for the pressure in Ω (left) and Γ (right) for triangular and polygonal grids.

4. NUMERICAL RESULTS

In this section we present some numerical tests to assess the theoretical results presented in the previous sections and to illustrate the behavior of the numerical method on more complex cases.

4.1. Convergence test

To verify the theoretical order of convergence we consider a test case inspired by [10]. The domain is the square $\Omega = [-1, 1] \times [-1, 1]$, and in our case the geometry has been slightly modified to assess the behavior of the numerical method in the presence of an immersed fracture, $\Gamma = [-0.9, 0.9] \times \{0\}$ of aperture $l_\Gamma = 0.01$. We consider a constant and isotropic permeability, equal to one in the fracture and in the surrounding medium, and we impose a volumetric source term only in the fracture, i.e. $f(x, y) = 0$ and $\hat{f} = l_\Gamma \cos(x)$. On the whole boundary $\partial\Omega$ we set Dirichlet boundary conditions with $g_P = \cos(x)\cosh(y)$, while at the tips of the fracture we set non-homogeneous Neumann boundary conditions, $\hat{g}_\mathbf{u} = l_\Gamma \sin(x)$. The exact solution is then

$$p = \begin{cases} \cos(x)\cosh(y) & \text{in } \Omega \\ \cos(x) & \text{in } \Gamma. \end{cases}$$

We have performed this test both on unstructured triangular grids and general polygonal grids with different resolutions. Polygonal grids have been generated from triangular grids by means of random merging of neighboring triangles. Since the contribution of the fracture to the absolute error in the pressure defined by (85) is much smaller with respect to the contribution of the surrounding medium, it is presented separately for the sake of clarity, see figure 4. We can observe superconvergence of the pressure (order h^2 instead of h) both for the triangular and the polygonal grid case. As concerns the error in the velocity, defined as in (83), it decreases with order h as expected (figure 5). In this case the experimental order is slightly higher for triangular grids with respect to more general ones, in particular 1.3471 versus 1.0662.

4.2. Test on the theoretical bound for ξ_0

To perform meaningful experiments on the coupling conditions (4) we designed a test case such that $[\![\mathbf{u}\cdot\mathbf{n}]\!] \neq 0$ on Γ. In particular, we consider a square domain $\Omega = [0, 1] \times [0, 1]$, cut by an horizontal fracture $\Gamma = [0, 1] \times \{0\}$ of aperture $l_\Gamma = 0.01$. The boundary conditions are depicted in figure 6, and no source term is considered in the

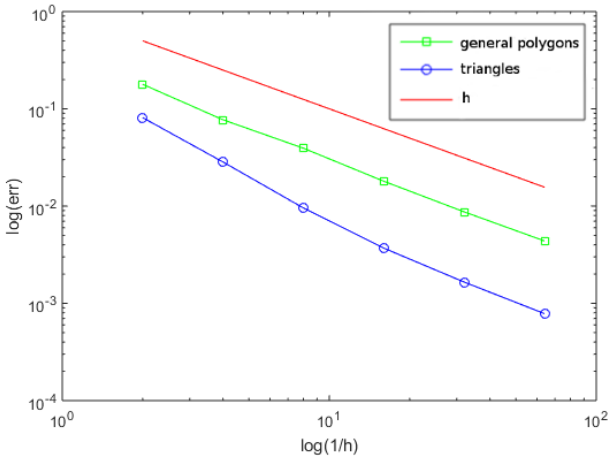

FIGURE 5. Relative error for the velocity in Ω for triangular and polygonal grids.

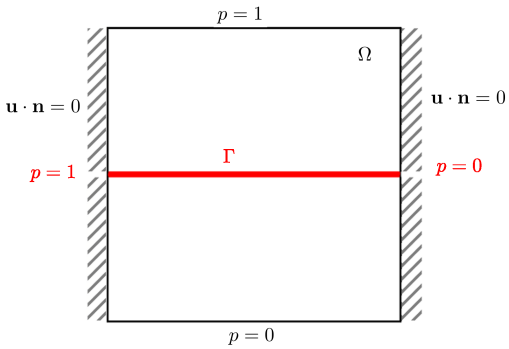

FIGURE 6. Domain and boundary conditions for test case 4.2

fracture nor in the bulk: note that due to the asymmetric boundary conditions there is flow along the fracture. We have set $\mathbf{K} = \mathbb{I}$, $K_\tau = 1$, $K_n = 0.01$.

As discussed in section 3.6.1, even if in the case $\xi_0 = 0$ the continuous problem is not well posed, it can be shown that this choice of the parameter is possible in the discrete case, and in particular ξ_0 should be chosen according to inequality (70). In practice, for any mesh size, ξ_0 can be taken equal to zero, as proven by the results in figure 7: if $\xi_0 < 0$ the pressure solution violates the maximum principle, while for $\xi_0 = 0$ we obtain the correct solution. Moreover, as shown in figure 8, in this latter case the pressure in the fracture is exactly the average of the pressure on the two sides of the fracture.

We have computed the minimum eigenvalue of the matrix A_h for different values of ξ_0 and different grid resolutions to verify the inequality (70): negative eigenvalues indicate that A_h is not positive definite and may correspond to solutions that violate the maximum principle as summarized in Table 1. Note that the minimum acceptable ξ_0 is smaller for coarse grid, while for more refined grids we approach the theoretical limits of the continuous problem: however, for $h > 0$ $\xi_0 = 0$ is always acceptable.

4.3. **A completely immersed network**

To conclude, we consider a more complex case where a network of six fractures of aperture $l_\Gamma = 0.01$ is completely immersed in the domain Ω. Homogeneous Dirichlet boundary conditions are imposed on $\partial\Omega$, while

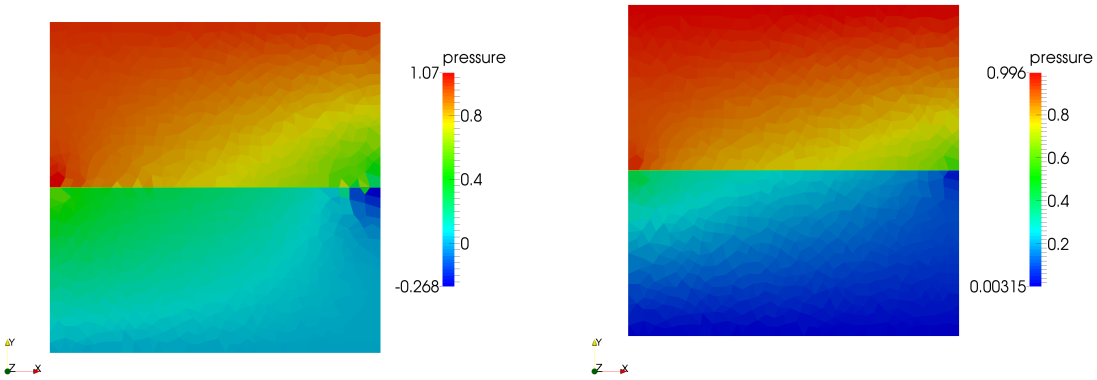

FIGURE 7. Pressure in the domain for $\xi_0 = -0.05$ (left) and $\xi_0 = 0$ (right)

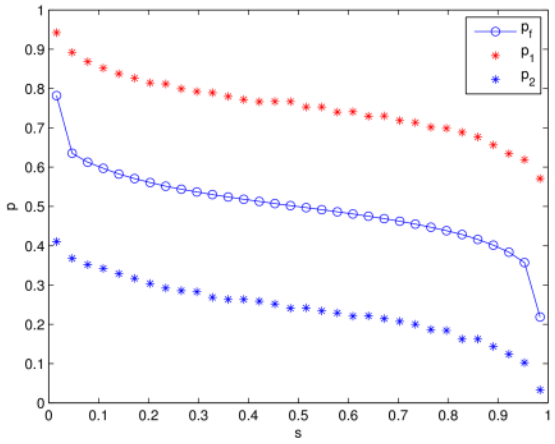

FIGURE 8. Pressure in the fracture for $\xi_0 = 0$, and pressure in Ω on the two sides of the fracture. Here s denotes the curvilinear abscissa of the fracture.

	ξ_0	-0.5	-0.25	-0.05	-0.02	0	0.05	0.25	0.5
h=0.1	$\min \lambda_A$	-2.98e-2	-1.42e-2	-1.70e-3	1.61e-4	1.40e-3	1.50e-3	1.50e-3	1.50e-3
	$\min_{\Omega\cup\Gamma} p_h$	-1.02e-3	-2.29e0	1.01e-2	1.01e-2	1.01e-2	1.02e-2	1.02e-2	1.03e-2
	$\max_{\Omega\cup\Gamma} p_h$	1.04e0	4.14e0	9.89e-1	9.89e-1	9.89e-1	9.89e-1	9.89e-1	9.89e-1
h=0.05	$\min \lambda_A$	-1.53e-2	-7.50e-3	-1.20e-3	-2.89e-4	3.17e-4	3.30e-4	3.30e-4	3.30e-4
	$\min_{\Omega\cup\Gamma} p_h$	-3.49e-2	-8.95e-1	-2.68e-1	-3.27e-3	3.15e-3	3.41e-3	3.41e-3	3.41e-3
	$\max_{\Omega\cup\Gamma} p_h$	1.03e0	1.92e0	1.07e0	9.96e-1	9.96e-1	9.96e-1	9.96e-1	9.96e-1

TABLE 1. Minimum eigenvalue of A_h and corresponding extrema of pressure for two different grid sizes.

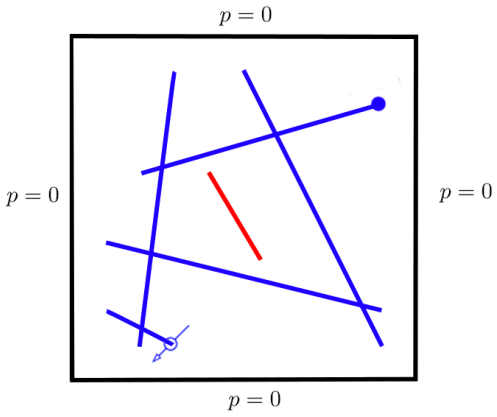

FIGURE 9. Domain and boundary conditions for test case 4.3. The fractures highlighted in blue are more permeable than the matrix, while the red one is locking. The injection and production wells are located at two fracture tips.

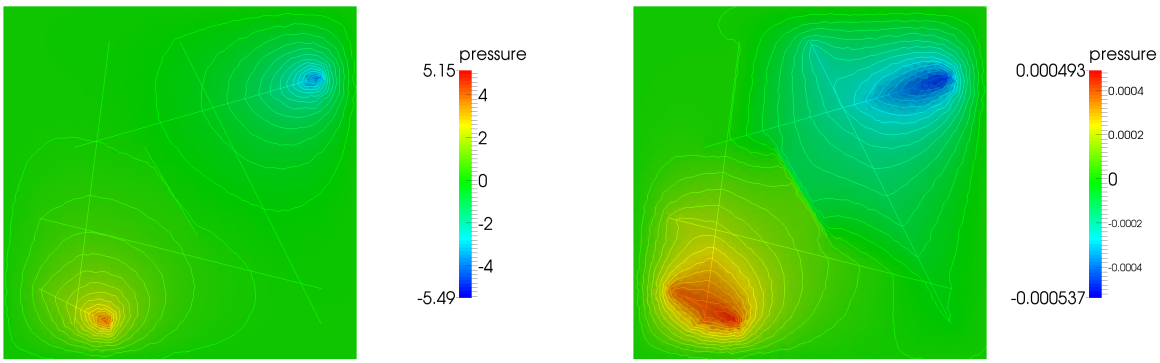

FIGURE 10. Pressure fields for test case 4.3 for two values of the contrast ϵ: $\epsilon_1 = 1.0e1$ on the left, $\epsilon_2 = 1.0e6$ on the right.

no flow is imposed at the fracture tips, except for the two, marked in figure 9, where injection and production are mimicked with Neumann boundary conditions of inflow/outflow respectively. Five fractures are more permeable of the surrounding medium, with $K_\tau = K_n = \epsilon$, while the fracture at the center of the domain, marked in red in figure 9 is blocking, with $K_\tau = K_n = \epsilon^{-1}$. We set $K = \mathbb{I}$ in the porous medium and consider two cases, with $\epsilon = \epsilon_1 = 1.0e1$ and $\epsilon = \epsilon_2 = 1.0e6$. The results are shown in figure 10. In both cases the effect of permeable and blocking fractures is visible on the pressure isolines. In the case of lower contrast, $\epsilon = \epsilon_1$, the matrix/fracture system is overall less permeable and pressure reaches higher values. In the case $\epsilon = \epsilon_2$ the injected fluid flow preferably in the connected fractures and the pressure isolines are clearly stretched in the direction of the fractures.

5. Conclusions

In this work we presented, for the first time at the best of our knowledge, a well-posedness results for Darcy's flow in fractured media in mixed form where pressure is not imposed on part of the boundary of the fracture network. We have also given a full analysis of a mimetic finite difference approximation for the problem.

The theory has been set for a general 3D or 2D problem, even if the numerical experiments rely on the 2D case. Work on implementing a full 3D code is under way.

Several extensions may be planned. For instance, one may consider time dependent problems and different models for the flow in the fracture network (for instance Brinkman or Stokes models). The good approximation of the flow field given by the mixed formulation could be useful for the coupling with an advection-diffusion problem.

Moving to multi-phase flow opens the question of the proper interface conditions for the saturation equation and how to implement them in the context of mimetic finite differences.

We mention that our analysis could be the basis for a more general study of polygonal discretization based on virtual element methods, which could open a possibility of implementing higher order approximations.

In the numerical experiments the governing linear system has been solved using direct multi-frontal methods. This will not be possible, in general, for 3D problems. The use of iterative schemes opens up the issue of finding optimal preconditioners, particularly when the permeability is strongly heterogeneous.

6. Acknowledgments

The authors gratefully acknowledge Paola Antonietti and Marco Verani for many fuitful discussions. This work is part of a research activity of the computational geoscience group of the MOX laboratory of Politecnico di Milano (`compgeo.mox.polimi.it`) on numerical schemes for flow in fractured porous media.

The authors wish also to thank the anonymous reviewers whose comments helped to improve the manuscript.

References

[1] P. Adler, J.-F. Thovert, and V. Mourzenko. *Fractured Porous Media*. Oxford University Press, 2013.

[2] O. Al-Hinai, S. Srinivasan, and M. F. Wheeler. Mimetic finite differences for flow in fractures from microseismic data. In *SPE Reservoir Simulation Symposium, 23-25 February, Houston, Texas, USA*. Society of Petroleum Engineers, 2015.

[3] C. Alboin, J. Jaffré, J. E. Roberts, X. Wang, and C. Serres. *Domain decomposition for some transmission problems in flow in porous media*, volume 552 of *Lecture Notes in Phys.*, pages 22–34. Springer, Berlin, 2000.

[4] P. Angot, F. Boyer, and F. Hubert. Asymptotic and numerical modelling of flows in fractured porous media. *M2AN Math. Model. Numer. Anal.*, 43(2):239–275, 2009.

[5] P. Antonietti, L. Beirão da Veiga, N. Bigoni, and M. Verani. Mimetic finite differences for nonlinear and control problems. *Math. Models Methods Appl. Sci.*, 24(8):1457–1493, 2014.

[6] P. Antonietti, C. Facciolà, A. Russo, and M. Verani. Discontinuous Galerkin approximation of flows in fractured porous media. Technical Report 22/2016, MOX, Politecnico di Milano, 2016.

[7] P. F. Antonietti, L. Beirão da Veiga, and M. Verani. A mimetic discretization of elliptic obstacle problems. *Math. Comp.*, 82(283):1379–1400, 2013.

[8] P. F. Antonietti, N. Bigoni, and M. Verani. Mimetic discretizations of elliptic control problems. *J. Sci. Comput.*, 56(1):14–27, 2013.

[9] P. F. Antonietti, N. Bigoni, and M. Verani. Mimetic finite difference approximation of quasilinear elliptic problems. *Calcolo*, 52(1):45–67, 2015.

[10] P. F. Antonietti, L. Formaggia, A. Scotti, M. Verani, and N. Verzotti. Mimetic finite difference approximation of flows in fractured porous media. *ESAIM: M2AN*, 50(3):809–832, 2016.

[11] T. Arbogast, J. Douglas, Jr, and U. Hornung. Derivation of the double porosity model of single phase flow via homogenization theory. *SIAM Journal on Mathematical Analysis*, 21(4):823–836, 1990.

[12] M. F. Benedetto, S. Berrone, S. Pieraccini, and S. Scialò. The virtual element method for discrete fracture network simulations. *Comput. Methods Appl. Mech. Engrg.*, 280:135–156, 2014.

[13] M. F. Benedetto, S. Berrone, and S. Scialò. A globally conforming method for solving flow in discrete fracture networks using the virtual element method. *Finite Elements in Analysis and Design*, 109:23– 36, 2016.

[14] B. Berkowitz. Characterizing flow and transport in fractured geological media: A review. *Advances in Water Resources*, 25(8-12):861–884, 2002.

[15] D. Boffi, F. Brezzi, and M. Fortin. *Mixed finite element methods and applications*, volume 44 of *Springer Series in Computational Mathematics*. Springer, Heidelberg, 2013.
[16] W. Boon and J. Nordbotten. Robust Discretization of Flow in Fractured Porous Media. *Arxiv preprint*, (arXiv:1601.06977), 2016.
[17] K. Brenner, J. Hennicker, R. Masson, and P. Samier. Gradient discretization of hybrid dimensional Darcy flows in fractured porous media with discontinuous pressures at the matrix fracture interfaces. *IMA J Numer Anal*, (on line), 2016. doi:10.1093/imanum/drw044.
[18] S. Brenner and L. Scott. *The mathematical theory of finite element methods*. Springer, Berlin/Heidelberg, 1994.
[19] F. Brezzi, K. Lipnikov, and M. Shashkov. Convergence of the mimetic finite difference method for diffusion problems on polyhedral meshes. *SIAM Journal on Numerical Analysis*, 43(5):1872–1896, 2006.
[20] F. Brezzi, K. Lipnikov, M. Shashkov, and V. Simoncini. A new discretization methodology for diffusion problems on generalized polyhedral meshes. *Comput. Methods Appl. Mech. Engrg.*, 196(37-40):3682–3692, 2007.
[21] L. B. Da Veiga, K. Lipnikov, and G. Manzini. Convergence analysis of the high-order mimetic finite difference method. *Numerische Mathematik*, 113(3):325–356, 2009.
[22] B. da Veiga Lourenco, K. Lipnikov, and G. Manzini. *The mimetic finite difference method for elliptic problems*, volume 11 of *MS&A. Modeling, Simulation and Applications*. Springer, Cham, 2014.
[23] C. D'Angelo and A. Scotti. A mixed finite element method for Darcy flow in fractured porous media with non-matching grids. *ESAIM: Mathematical Modelling and Numerical Analysis*, 46(02):465–489, 2012.
[24] F. Dassi, S. Perotto, L. Formaggia, and P. Ruffo. Efficient geometric reconstruction of complex geological structures. *Mathematics and Computers in Simulation*, 2014.
[25] I. Faille, A. Fumagalli, J. Jaffré, and J. E. Roberts. Model reduction and discretization using hybrid finite volumes for flow in porous media containing faults. *Computational Geosciences*, 20(2):317–339, 2016.
[26] L. Formaggia, A. Fumagalli, A. Scotti, and P. Ruffo. A reduced model for Darcy's problem in networks of fractures. *ESAIM: Mathematical Modelling and Numerical Analysis*, 48(4):1089–1116, 2014.
[27] A. Fumagalli and E. Keilegavlen. Dual virtual element method for discrete fractures networks. *arXiv preprint*, (arXiv:1610.02905), 2016.
[28] A. Fumagalli and A. Scotti. A reduced model for flow and transport in fractured porous media with non-matching grids. In *Proceedings of ENUMATH 2011, the 9th European Conference on Numerical Mathematics and Advanced Applications, Springer-Verlag*, 2012.
[29] A. Fumagalli and A. Scotti. A numerical method for two-phase flow in fractured porous media with non-matching grids. *Advances in Water Resources*, 62, Part C(0):454–464, 2013. Computational Methods in Geologic CO2 Sequestration.
[30] A. Fumagalli and A. Scotti. An efficient XFEM approximation of Darcy flows in arbitrarily fractured porous media. *Oil & Gas Science and Technology–Revue dIFP Energies nouvelles*, 69(4):555–564, 2014.
[31] H. Huang, T. A. Long, J. Wan, and W. P. Brown. On the use of enriched finite element method to model subsurface features in porous media flow problems. *Computational Geosciences*, 15(4):721–736, 2011.
[32] J. Jaffré, M. Mnejja, and J. E. Roberts. A discrete fracture model for two-phase flow with matrix-fracture interaction. *Procedia Computer Science*, 4:967–973, 2011.
[33] M. Karimi-Fard, L. Durlofsky, K. Aziz, et al. An efficient discrete-fracture model applicable for general-purpose reservoir simulators. *SPE Journal*, 9(02):227–236, 2004.
[34] B. Mallison, M. Hui, and W. Narr. Practical gridding algorithms for discrete fracture modeling workflows. In *12th European Conference on the Mathematics of Oil Recovery*, 2010.
[35] V. Martin, J. Jaffré, and J. E. Roberts. Modeling fractures and barriers as interfaces for flow in porous media. *SIAM Journal on Scientific Computing*, 26(5):1667–1691, 2005.
[36] N. Schwenck, B. Flemisch, R. Helmig, and B. I. Wohlmuth. Dimensionally reduced flow models in fractured porous media: crossings and boundaries. *Computational Geosciences*, 19(6):1219–1230, 2015.